

Thermalization of magnons in yttrium-iron garnet: nonequilibrium functional renormalization group approach

Johannes Hick,¹ Thomas Kloss,² and Peter Kopietz¹

¹*Institut für Theoretische Physik, Universität Frankfurt,
Max-von-Laue Strasse 1, 60438 Frankfurt, Germany*

²*Laboratoire de Physique et Modélisation des Milieux Condensés,
CNRS and Université Joseph Fourier, 25 Avenue des Martyrs, 38042 Grenoble, France*

(Dated: August 09, 2012)

Using a nonequilibrium functional renormalization group (FRG) approach we calculate the time evolution of the momentum distribution of a magnon gas in contact with a thermal phonon bath. As a cutoff for the FRG procedure we use a hybridization parameter Λ giving rise to an artificial damping of the phonons. Within our truncation of the FRG flow equations the time evolution of the magnon distribution is obtained from a rate equation involving cutoff-dependent nonequilibrium self-energies, which in turn satisfy FRG flow equations depending on cutoff-dependent transition rates. Our approach goes beyond the Born collision approximation and takes the feedback of the magnons on the phonons into account. We use our method to calculate the thermalization of a quasi two-dimensional magnon gas in the magnetic insulator yttrium-iron garnet after a highly excited initial state has been generated by an external microwave field. We obtain good agreement with recent experiments.

PACS numbers: 05.30.Jp, 05.10.Cc, 75.30.Ds

I. INTRODUCTION

Calculating the nonequilibrium time evolution of interacting many-body systems is a challenging problem which usually requires advanced many body methods and serious numerical calculations. This problem is of interest in many different fields¹, including ultracold atoms², collision experiments of heavy nuclei³, exciton-polariton systems in semiconductor microcavities⁴, dissipative quantum systems⁵ and pumped magnon gases in magnetic insulators^{6,7}. The nonequilibrium dynamics of weakly interacting non-relativistic bosons has been successfully modeled by combining the Gross-Pitaevskii equation for the condensate with the Boltzmann equation for the quasi-particle excitations^{8,9}. However, the collision integral in the Boltzmann equation is usually calculated only perturbatively to second order in the bare interaction. This approximation breaks down for strong interactions or for high densities, so that it is important to develop non-perturbative methods. For N -component relativistic scalar field theories Berges and co-authors¹⁰ have recently shown by means of a two-particle irreducible resummed large- N expansion that vertex corrections (which are neglected in the Boltzmann equation) qualitatively change the scaling behavior of the momentum distribution for small momenta.

An alternative non-perturbative method to deal with strongly correlated systems out of equilibrium is based on the functional renormalization group (FRG)^{11–15}. Recently, several authors have used nonequilibrium FRG methods to calculate the time evolution of various types of many body systems^{16–18}. It turns out, however, that the proper implementation of nonequilibrium FRG schemes depends on the specific problem of interest; in fact, many technical problems (such as the choice of the

cutoff parameter, or the construction of sensible approximation strategies which respect causality and the conservation laws) have to be solved in order to turn the nonequilibrium FRG into a useful and competitive calculational tool.

In this work we shall develop a particular implementation of the nonequilibrium FRG which is suited to study time-dependent nonequilibrium phenomena in Bose systems in contact with a thermal phonon bath. To be specific, we identify the bosons with the magnons (i.e., quantized spin-waves) in a ferromagnetic insulator; however the methods developed in this work are also useful to calculate the nonequilibrium time evolution of any non-relativistic Bose gas. Moreover, by means of a straightforward modification of our method it should also be possible to study Fermi gases out of equilibrium. The Hamiltonian of our system is

$$\mathcal{H} = \sum_{\mathbf{k}} \epsilon_{\mathbf{k}} a_{\mathbf{k}}^{\dagger} a_{\mathbf{k}} + \sum_{\mathbf{q}} \omega_{\mathbf{q}} b_{\mathbf{q}}^{\dagger} b_{\mathbf{q}} + \frac{1}{\sqrt{V}} \sum_{\mathbf{q}} \gamma_{\mathbf{q}} \rho_{-\mathbf{q}} (b_{\mathbf{q}} + b_{-\mathbf{q}}^{\dagger}), \quad (1.1)$$

where $a_{\mathbf{k}}^{\dagger}$ creates a magnon with momentum \mathbf{k} and energy $\epsilon_{\mathbf{k}}$, while $b_{\mathbf{q}}^{\dagger}$ creates an acoustic phonon with momentum \mathbf{q} and energy $\omega_{\mathbf{q}} = c|\mathbf{q}|$. The volume of the system is denoted by V , the operator $\rho_{\mathbf{q}} = \sum_{\mathbf{k}} a_{\mathbf{k}}^{\dagger} a_{\mathbf{k}+\mathbf{q}}$ represents Fourier components of the magnon density, and the magnon-phonon coupling $\gamma_{\mathbf{q}}$ is assumed to be proportional to $\sqrt{\omega_{\mathbf{q}}}$, which is a simple consequence of the fact that density fluctuations associated with the creation of longitudinal phonons are proportional to the divergence of the corresponding displacement field¹⁹.

A model Hamiltonian of the form (1.1) has been used previously by Bányai *et al.*²⁰ to describe the kinetics of

Bose-Einstein condensation of excitons. In Sec. II we will review the rate equation approach adopted by these authors. Here we use the model Hamiltonian (1.1) to study the nonequilibrium dynamics of magnons in thin stripes of the magnetic insulator yttrium-iron garnet (YIG)²¹. The time evolution of the momentum distribution of magnons in YIG has been studied experimentally by means of the method of Brillouin light scattering^{6,22,23}. Note that the effective magnon Hamiltonian of YIG is of the form (1.1) if we identify the operators $a_{\mathbf{k}}^{\dagger}$ with the creation operators of the relevant magnon band in YIG²⁴. In the experimentally realized thin stripe geometry the magnons form a quasi two-dimensional weakly interacting Bose gas. If the external magnetic field \mathbf{H} is aligned along the stripe axis and the angle $\theta_{\mathbf{k}}$ between the magnetic field and the magnon momentum \mathbf{k} is not too large, the long-wavelength energy dispersion of the experimentally relevant magnon band in YIG can be approximated by^{24,25}

$$\epsilon_{\mathbf{k}} = [h + \rho_{\text{ex}}\mathbf{k}^2 + \Delta(1 - f_{\mathbf{k}})\sin^2\theta_{\mathbf{k}}]^{1/2} \times [h + \rho_{\text{ex}}\mathbf{k}^2 + \Delta f_{\mathbf{k}}]^{1/2}. \quad (1.2)$$

Here $h = \mu|\mathbf{H}|$ is the Zeeman energy associated with the external magnetic field (μ is the magnetic moment of the localized spins in YIG), ρ_{ex} is the exchange spin-stiffness, and the energy Δ is the characteristic energy scale associated with dipole-dipole interactions in YIG. To describe the experiments it is sufficient to retain only a single magnon band and work with an effective two-dimensional model. The form factor $f_{\mathbf{k}}$ in Eq. (1.2) can then be approximated by²⁴

$$f_{\mathbf{k}} \approx \frac{1 - e^{-|\mathbf{k}|d}}{|\mathbf{k}|d}, \quad (1.3)$$

where d is the transverse thickness of the YIG stripe. As will be discussed in more detail in Sec. IV, the parameters ρ_{ex} , Δ and d entering the magnon dispersion (1.2) are all known from experiment, so that we may use our model Hamiltonian (1.1) to make specific predictions of the nonequilibrium dynamics of the magnon gas in YIG.

Note that our Hamiltonian (1.1) does not contain direct two-body interactions between the magnons, so that in the absence of phonons the magnons do not interact. A more realistic model describing the Bose-Einstein condensation of magnons in YIG should also include many-body interactions between the magnons^{21,26}. Although these interactions compete with the phonons to thermalize the magnon gas, we focus here on a regime where the dominant thermalization mechanism is due to magnon-phonon scattering.

II. RATE EQUATIONS FROM THE KELDYSH TECHNIQUE

The nonequilibrium dynamics of a boson Hamiltonian of the type (1.1) with quadratic boson dispersion $\epsilon_{\mathbf{k}}$ has

been studied in Ref. [20] using a simple decoupling procedure of the equations of motion, which yields the following rate equation for the time-dependent momentum distribution $n_{\mathbf{k}}(t) = \langle a_{\mathbf{k}}^{\dagger}(t)a_{\mathbf{k}}(t) \rangle$,

$$\partial_t n_{\mathbf{k}}(t) = \frac{1}{V} \sum_{\mathbf{k}'} \left\{ [1 + n_{\mathbf{k}}(t)] W_{\mathbf{k},\mathbf{k}'} n_{\mathbf{k}'}(t) - [1 + n_{\mathbf{k}'}(t)] W_{\mathbf{k}',\mathbf{k}} n_{\mathbf{k}}(t) \right\}. \quad (2.1)$$

The transition rates are given by Fermi's golden rule²⁷

$$W_{\mathbf{k},\mathbf{k}'} = 2\gamma_{\mathbf{k}-\mathbf{k}'}^2 b(\epsilon_{\mathbf{k}} - \epsilon_{\mathbf{k}'}) D_{\mathbf{k}-\mathbf{k}'}^I(\epsilon_{\mathbf{k}} - \epsilon_{\mathbf{k}'}), \quad (2.2)$$

where the Bose function

$$b(\omega) = \frac{1}{e^{\beta\omega} - 1} \quad (2.3)$$

is the equilibrium distribution of the phonon bath at temperature $T = 1/\beta$, and

$$D_q^I(\omega) = \pi \text{sgn}(\omega) [\delta(\omega - \omega_q) + \delta(\omega + \omega_q)] \quad (2.4)$$

is the spectral function of the symmetrized phonon propagator, see Eq. (C4c) in Appendix C. Note that for negative frequencies the spectral function (2.4) is negative, which is a general property of any bosonic spectral function²⁸. Using the fact that $D_q^I(-\omega) = -D_q^I(\omega)$ and $b(-\omega) = -[1 + b(\omega)] = -e^{\beta\omega}b(\omega)$ one easily verifies that the transition rates satisfy detailed balance²⁷

$$W_{\mathbf{k},\mathbf{k}'} e^{-\beta\epsilon_{\mathbf{k}'}} = W_{\mathbf{k}',\mathbf{k}} e^{-\beta\epsilon_{\mathbf{k}}}. \quad (2.5)$$

Numerical solutions of Eq. (2.1) for finite systems of bosons with quadratic dispersion can be found in Ref. [20]. However, for finite systems the Dirac δ -functions in the transition rates (2.2) lead to singular results. Bányai *et al.*²⁰ therefore replace the δ -functions (by hand) by Lorentzians of finite width, thus introducing an additional phenomenological parameter into the problem. This is somewhat unsatisfactory, because the final results can be sensitive to the width of the broadened δ -functions. Here we present an alternative solution to this problem: within our FRG approach with hybridization cutoff it is straightforward to take the physical broadening of the phonon propagators due to the coupling to the magnon system self-consistently into account.

To obtain a FRG generalization of the rate equation (2.1), an approach based on the decoupling of the equations of motion is not useful; instead, the nonequilibrium problem should be formulated in terms of self-energies which are obtained via functional integral techniques. Before developing the nonequilibrium FRG approach, it is therefore instructive to carefully re-derive the rate equation (2.1) using the functional integral formulation of the Keldysh method^{9,29}. Let us therefore recall that in the Keldysh method the nonequilibrium distribution function $n_{\mathbf{k}}(t)$ is related to the Keldysh Green function at equal times,

$$iG_{\mathbf{k}}^K(t, t) = 1 + 2n_{\mathbf{k}}(t). \quad (2.6)$$

In order to calculate this, one has to consider $G_{\mathbf{k}}^K(t, t')$ together with the retarded and the advanced Green functions,

$$iG_{\mathbf{k}}^R(t, t') = \Theta(t - t') \langle [a_{\mathbf{k}}(t), a_{\mathbf{k}}^\dagger(t')] \rangle, \quad (2.7a)$$

$$iG_{\mathbf{k}}^A(t, t') = -\Theta(t' - t) \langle [a_{\mathbf{k}}(t), a_{\mathbf{k}}^\dagger(t')] \rangle, \quad (2.7b)$$

$$iG_{\mathbf{k}}^K(t, t') = \langle \{a_{\mathbf{k}}(t), a_{\mathbf{k}}^\dagger(t')\} \rangle, \quad (2.7c)$$

where $[,]$ is the commutator and $\{ , \}$ is the anticommutator. The corresponding phonon Green functions are

$$iF_{\mathbf{q}}^R(t, t') = \Theta(t - t') \langle [b_{\mathbf{q}}(t), b_{\mathbf{q}}^\dagger(t')] \rangle, \quad (2.8a)$$

$$iF_{\mathbf{q}}^A(t, t') = -\Theta(t' - t) \langle [b_{\mathbf{q}}(t), b_{\mathbf{q}}^\dagger(t')] \rangle, \quad (2.8b)$$

$$iF_{\mathbf{q}}^K(t, t') = \langle \{b_{\mathbf{q}}(t), b_{\mathbf{q}}^\dagger(t')\} \rangle. \quad (2.8c)$$

Since the magnons in Eq. (1.1) couple only to the hermitian combination

$$X_{\mathbf{q}} = \frac{1}{\sqrt{2}} (b_{\mathbf{q}} + b_{-\mathbf{q}}^\dagger) \quad (2.9)$$

of the phonon fields, it is convenient to define

$$iD_{\mathbf{q}}^R(t, t') = \Theta(t - t') \langle [X_{\mathbf{q}}(t), X_{-\mathbf{q}}(t')] \rangle, \quad (2.10a)$$

$$iD_{\mathbf{q}}^A(t, t') = -\Theta(t' - t) \langle [X_{\mathbf{q}}(t), X_{-\mathbf{q}}(t')] \rangle, \quad (2.10b)$$

$$iD_{\mathbf{q}}^K(t, t') = \langle \{X_{\mathbf{q}}(t), X_{-\mathbf{q}}(t')\} \rangle. \quad (2.10c)$$

Following Kamenev^{9,29}, we represent the above Green functions as functional averages,

$$iG_{\mathbf{k}}^R(t, t') = \langle a_{\mathbf{k}}^C(t) \bar{a}_{\mathbf{k}}^Q(t') \rangle \equiv iG_{\mathbf{k}}^{CQ}(t, t'), \quad (2.11a)$$

$$iG_{\mathbf{k}}^A(t, t') = \langle a_{\mathbf{k}}^Q(t) \bar{a}_{\mathbf{k}}^C(t') \rangle \equiv iG_{\mathbf{k}}^{QC}(t, t'), \quad (2.11b)$$

$$iG_{\mathbf{k}}^K(t, t') = \langle a_{\mathbf{k}}^C(t) \bar{a}_{\mathbf{k}}^C(t') \rangle \equiv iG_{\mathbf{k}}^{CC}(t, t'), \quad (2.11c)$$

and similarly for the phonon Green functions,

$$iF_{\mathbf{q}}^R(t, t') = \langle b_{\mathbf{q}}^C(t) \bar{b}_{\mathbf{q}}^Q(t') \rangle \equiv iF_{\mathbf{q}}^{CQ}(t, t'), \quad (2.12a)$$

$$iF_{\mathbf{q}}^A(t, t') = \langle b_{\mathbf{q}}^Q(t) \bar{b}_{\mathbf{q}}^C(t') \rangle \equiv iF_{\mathbf{q}}^{QC}(t, t'), \quad (2.12b)$$

$$iF_{\mathbf{q}}^K(t, t') = \langle b_{\mathbf{q}}^C(t) \bar{b}_{\mathbf{q}}^C(t') \rangle \equiv iF_{\mathbf{q}}^{CC}(t, t'). \quad (2.12c)$$

The functional averages are defined as

$$\langle a_{\mathbf{k}}^\lambda(t) \bar{a}_{\mathbf{k}}^{\lambda'}(t') \rangle = \int \mathcal{D}[\bar{a}, a, \bar{b}, b] e^{iS[\bar{a}, a, \bar{b}, b]} a_{\mathbf{k}}^\lambda(t) \bar{a}_{\mathbf{k}}^{\lambda'}(t'), \quad (2.13)$$

and similarly for $\langle b_{\mathbf{q}}^\lambda(t) \bar{b}_{\mathbf{q}}^{\lambda'}(t') \rangle$. The superscripts $\lambda, \lambda' \in \{C, Q\}$ label the classical (C) and quantum (Q) components of the fields, which are related to the contour components $a_{\mathbf{k}}^\pm(t)$ and $b_{\mathbf{k}}^\pm(t)$ via³⁰

$$a_{\mathbf{k}}^C(t) = \frac{1}{\sqrt{2}} [a_{\mathbf{k}}^+(t) + a_{\mathbf{k}}^-(t)], \quad (2.14a)$$

$$a_{\mathbf{k}}^Q(t) = \frac{1}{\sqrt{2}} [a_{\mathbf{k}}^+(t) - a_{\mathbf{k}}^-(t)], \quad (2.14b)$$

$$b_{\mathbf{k}}^C(t) = \frac{1}{\sqrt{2}} [b_{\mathbf{k}}^+(t) + b_{\mathbf{k}}^-(t)], \quad (2.14c)$$

$$b_{\mathbf{k}}^Q(t) = \frac{1}{\sqrt{2}} [b_{\mathbf{k}}^+(t) - b_{\mathbf{k}}^-(t)]. \quad (2.14d)$$

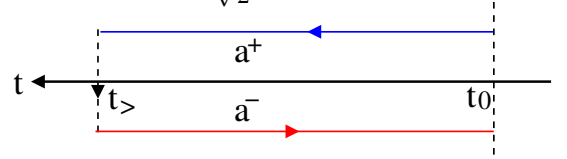


FIG. 1. (Color online) The Keldysh contour connects some initial time t_0 slightly above the real axis with some final time $t_>$ which is larger than all times of interest. It then crosses the real axis and goes back to t_0 slightly below the real axis. In accordance with the definition of time-ordering we draw later times to the left.

Here the superscripts \pm attached to the fields $a_{\mathbf{k}}^\pm(t)$ and $b_{\mathbf{k}}^\pm(t)$ refer to the upper and lower branch of the Keldysh contour shown in Fig. 1. The Keldysh action is given by

$$\begin{aligned} S[\bar{a}, a, \bar{b}, b] = & \int dt \int dt' \left\{ \sum_{\mathbf{k}} (\bar{a}_{\mathbf{k}}^C(t), \bar{a}_{\mathbf{k}}^Q(t)) \begin{pmatrix} 0 & (\hat{G}_0^A)^{-1} \\ (\hat{G}_0^R)^{-1} & -(\hat{G}_0^R)^{-1} \hat{G}_0^K (\hat{G}_0^A)^{-1} \end{pmatrix}_{tt'} \begin{pmatrix} a_{\mathbf{k}}^C(t') \\ a_{\mathbf{k}}^Q(t') \end{pmatrix} \right. \\ & \left. + \sum_{\mathbf{q}} (\bar{b}_{\mathbf{q}}^C(t), \bar{b}_{\mathbf{q}}^Q(t)) \begin{pmatrix} 0 & (\hat{F}_0^A)^{-1} \\ (\hat{F}_0^R)^{-1} & -(\hat{F}_0^R)^{-1} \hat{F}_0^K (\hat{F}_0^A)^{-1} \end{pmatrix}_{tt'} \begin{pmatrix} b_{\mathbf{q}}^C(t') \\ b_{\mathbf{q}}^Q(t') \end{pmatrix} \right\} \\ & - \int dt \frac{1}{\sqrt{V}} \sum_{\mathbf{k}, \mathbf{q}} \gamma_{\mathbf{q}} \left[(\bar{a}_{\mathbf{k}+\mathbf{q}}^C a_{\mathbf{k}}^Q + \bar{a}_{\mathbf{k}+\mathbf{q}}^Q a_{\mathbf{k}}^C) X_{\mathbf{q}}^C + (\bar{a}_{\mathbf{k}+\mathbf{q}}^C a_{\mathbf{k}}^C + \bar{a}_{\mathbf{k}+\mathbf{q}}^Q a_{\mathbf{k}}^Q) X_{\mathbf{q}}^Q \right]. \quad (2.15) \end{aligned}$$

Here we have defined the phonon fields

$$X_{\mathbf{q}}^\lambda(t) = \frac{1}{\sqrt{2}} [b_{\mathbf{q}}^\lambda(t) + \bar{b}_{-\mathbf{q}}^\lambda(t)] \quad , \quad \lambda = C, Q, \quad (2.16)$$

and \hat{G}_0^R, \hat{G}_0^A , and \hat{G}_0^K as well as \hat{F}_0^R, \hat{F}_0^A , and \hat{F}_0^K are infinite matrices in the time-labels (we omit for simplicity the momentum label), with matrix elements given by

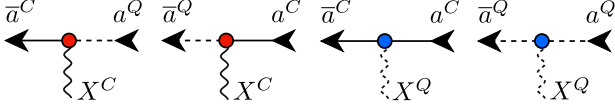


FIG. 2. (Color online) Graphical representation of the bare magnon-phonon vertices of the Keldysh action (2.15). Solid arrows pointing into the vertices represent a^C , while outgoing solid arrows represent \bar{a}^C . Dotted arrows represent the corresponding quantum components a^Q and \bar{a}^Q . Wavy solid lines represent the classical component X^C of the phonon field defined in Eq. (2.16), while wavy dotted lines represent the quantum component X^Q .

the Green functions (2.11a–2.12c) in the limit where the magnon-phonon coupling is switched off. A graphical representation of the interaction vertices in Eq. (2.15) is shown in Fig. 2. Note that the lower diagonal blocks of the inverse Gaussian propagators in Eq. (2.15) are actually infinitesimal regularizations of the continuous functional integral,

$$-(\hat{G}_0^R)^{-1}\hat{G}_0^K(\hat{G}_0^A)^{-1} = 2i\eta\hat{g}_0, \quad (2.17a)$$

$$-(\hat{F}_0^R)^{-1}\hat{F}_0^K(\hat{F}_0^A)^{-1} = 2i\eta\hat{f}_0, \quad (2.17b)$$

where \hat{g}_0 and \hat{f}_0 are diagonal matrices in the time labels which contain the magnon- and the phonon distribution functions in the non-interacting limit,

$$[\hat{g}_0]_{\mathbf{k},tt'} = \delta(t-t')g_{0,\mathbf{k}} = \delta(t-t')[1 + 2\langle a_{\mathbf{k}}^\dagger a_{\mathbf{k}} \rangle_0], \quad (2.18a)$$

$$[\hat{f}_0]_{\mathbf{q},tt'} = \delta(t-t')f_{0,\mathbf{q}} = \delta(t-t')[1 + 2\langle b_{\mathbf{q}}^\dagger b_{\mathbf{q}} \rangle_0]. \quad (2.18b)$$

Note that we restrict ourselves to initial states without correlations. Therefore the initial density matrix appears only via the initial conditions for the independent one- and two-point Green functions^{31–33}. Since the Keldysh action (2.15) is a Gaussian functional of the phonon fields, we may perform the integration over the phonon fields exactly and obtain the following effective Keldysh action for the magnon fields,

$$\begin{aligned} S[\bar{a}, a] = & \int dt \int dt' \sum_{\mathbf{k}} (\bar{a}_{\mathbf{k}}^C(t), \bar{a}_{\mathbf{k}}^Q(t)) \begin{pmatrix} 0 & (\hat{G}_0^A)^{-1} \\ (\hat{G}_0^R)^{-1} & -(\hat{G}_0^R)^{-1}\hat{G}_0^K(\hat{G}_0^A)^{-1} \end{pmatrix}_{tt'} \begin{pmatrix} a_{\mathbf{k}}^C(t') \\ a_{\mathbf{k}}^Q(t') \end{pmatrix} \\ & - \int dt \int dt' \frac{1}{V} \sum_{\mathbf{q}} \gamma_{\mathbf{q}}^2 \left\{ D_{0,\mathbf{q}}^R(t, t') \rho_{-\mathbf{q}}^{CQ}(t) [\rho_{\mathbf{q}}^{CC}(t') + \rho_{\mathbf{q}}^{QQ}(t')] + D_{0,\mathbf{q}}^A(t, t') [\rho_{-\mathbf{q}}^{CC}(t) + \rho_{-\mathbf{q}}^{QQ}(t)] \rho_{\mathbf{q}}^{QC}(t') \right. \\ & \left. + \frac{1}{2} D_{0,\mathbf{q}}^K(t, t') [\rho_{-\mathbf{q}}^{CQ}(t) + \rho_{-\mathbf{q}}^{QC}(t)] [\rho_{\mathbf{q}}^{CQ}(t') + \rho_{\mathbf{q}}^{QC}(t')] \right\}, \end{aligned} \quad (2.19)$$

where $D_{0,\mathbf{q}}^X(t, t')$, $X = R, A, K$, denote the non-interacting limit of the symmetrized phonon propagators defined in Eqs. (2.10a–2.10c), and we have defined

$$\rho_{\mathbf{q}}^{\lambda\lambda'}(t) = \sum_{\mathbf{k}} \bar{a}_{\mathbf{k}}^\lambda(t) a_{\mathbf{k}+\mathbf{q}}^{\lambda'}(t), \quad \lambda, \lambda' \in \{C, Q\}. \quad (2.20)$$

It is convenient to collect the retarded (\hat{G}^R), advanced (\hat{G}^A) and Keldysh (\hat{G}^K) components of the Green function into a matrix Green function,

$$\mathbf{G} = \begin{pmatrix} [\mathbf{G}]^{CC} & [\mathbf{G}]^{CQ} \\ [\mathbf{G}]^{QC} & 0 \end{pmatrix} = \begin{pmatrix} \hat{G}^K & \hat{G}^R \\ \hat{G}^A & 0 \end{pmatrix}, \quad (2.21)$$

whose inverse has the block structure

$$\mathbf{G}^{-1} = \begin{pmatrix} 0 & (\hat{G}^A)^{-1} \\ (\hat{G}^R)^{-1} & -(\hat{G}^R)^{-1}\hat{G}^K(\hat{G}^A)^{-1} \end{pmatrix}. \quad (2.22)$$

Defining the nonequilibrium self-energy via the matrix Dyson equation,

$$\mathbf{G}^{-1} = \mathbf{G}_0^{-1} - \Sigma, \quad (2.23)$$

we have in the Keldysh basis,

$$\Sigma = \begin{pmatrix} 0 & [\Sigma]^{CQ} \\ [\Sigma]^{QC} & [\Sigma]^{QQ} \end{pmatrix} = \begin{pmatrix} 0 & \hat{\Sigma}^A \\ \hat{\Sigma}^R & \hat{\Sigma}^K \end{pmatrix}, \quad (2.24)$$

with

$$\hat{\Sigma}^K = -[\mathbf{G}^{-1}]^{QQ} = (\hat{G}^R)^{-1}\hat{G}^K(\hat{G}^A)^{-1}. \quad (2.25)$$

By taking appropriate matrix elements of the nonequilibrium Dyson equation (2.23), we obtain a quantum kinetic equation for the distribution function. Actually, as reviewed in Appendix A, one can rewrite the kinetic equation in several different forms, depending on the choice of basis and on the re-shuffling of the terms in the Dyson equations. For our purpose, it is most convenient to parametrize the Keldysh block in terms of the distribution matrix \hat{g} by setting

$$\hat{G}^K = \hat{G}^R\hat{g}^\dagger - \hat{g}\hat{G}^A, \quad (2.26)$$

where in the non-interacting limit the matrix \hat{g} reduces to the non-interacting distribution matrix \hat{g}_0 given in

Eq. (2.18a). It is then easy to show (see Appendix A) that the Dyson equation (2.23) implies

$$-i(\hat{M}\hat{g} - \hat{g}^\dagger\hat{M}) = \hat{\Sigma}^{\text{in}} - \hat{\Sigma}^{\text{out}}, \quad (2.27)$$

where the infinite matrices \hat{M} , $\hat{\Sigma}^{\text{in}}$ and $\hat{\Sigma}^{\text{out}}$ can be written as

$$\hat{M} = \hat{M}_0 - \hat{\Sigma}^M, \quad (2.28)$$

$$\hat{\Sigma}^{\text{in}} = i\hat{\Sigma}^K, \quad (2.29)$$

$$\hat{\Sigma}^{\text{out}} = \frac{1}{2}(\hat{\Sigma}^I\hat{g} + \hat{g}^\dagger\hat{\Sigma}^I). \quad (2.30)$$

Here the matrix elements of \hat{M}_0 in the momentum-time basis are

$$[\hat{M}_0]_{\mathbf{k}t, \mathbf{k}'t'} = \delta_{\mathbf{k}, \mathbf{k}'} [i\delta'(t-t') - \epsilon_{\mathbf{k}}\delta(t-t')], \quad (2.31)$$

where $\delta'(t) = \frac{d}{dt}\delta(t)$ is the derivative of the Dirac δ -function. Moreover, we have introduced the mean (denoted by a superscript M) and the spectral (denoted by a superscript I for imaginary part) combinations of the retarded and advanced self-energies³⁴,

$$\hat{\Sigma}^M = \frac{1}{2}[\hat{\Sigma}^R + \hat{\Sigma}^A], \quad \hat{\Sigma}^I = i[\hat{\Sigma}^R - \hat{\Sigma}^A]. \quad (2.32)$$

Our notation for $\hat{\Sigma}^{\text{in}}$ and $\hat{\Sigma}^{\text{out}}$ anticipates that these quantities are related to the “in-scattering” and “out-scattering” contributions to the collision integral of the kinetic equation.

To describe the approach towards equilibrium, it is useful to express our kinetic equation in terms of Wigner transforms. Given any infinite matrix \hat{A} in the time labels with matrix elements $[\hat{A}]_{tt'}$, we define its Wigner transform $A(\tau; \omega)$ by performing a partial Fourier transformation with respect to the time difference $s = t - t'$,

$$A(\tau; \omega) = \int_{-\infty}^{\infty} ds e^{i\omega s} [\hat{A}]_{\tau+\frac{s}{2}, \tau-\frac{s}{2}}, \quad (2.33)$$

which is a function of the average time $\tau = \frac{t+t'}{2}$ and the frequency ω associated with the difference $t - t'$. The Wigner transform of our kinetic equation (2.27) is

$$\begin{aligned} & \partial_\tau \text{Reg}_{\mathbf{k}}(\tau; \omega) + 2(\omega - \epsilon_{\mathbf{k}}) \text{Im}g_{\mathbf{k}}(\tau; \omega) \\ & \quad + i(\hat{\Sigma}^M\hat{g} - \hat{g}^\dagger\hat{\Sigma}^M)_{(\tau; \omega)} \\ & = i\Sigma_{\mathbf{k}}^K(\tau; \omega) - \frac{1}{2}(\hat{\Sigma}^I\hat{g} + \hat{g}^\dagger\hat{\Sigma}^I)_{(\tau; \omega)}, \end{aligned} \quad (2.34)$$

where we have used the fact that the Wigner transform of \hat{g}^\dagger is given by the function $g^*(\tau; \omega)$, and $(\hat{A}\hat{B})_{(\tau; \omega)}$ denotes the Wigner transform of the product of two matrices in the time labels. Although in general such a product does not factorize into the product of Wigner transforms of \hat{A} and \hat{B} , there is an approximate factorization to leading order in a gradient expansion, see Eq. (A26). Assuming that such an expansion is justified, we obtain to leading order

$$i(\hat{\Sigma}^M\hat{g} - \hat{g}^\dagger\hat{\Sigma}^M)_{(\tau; \omega)} \approx -2\Sigma_{\mathbf{k}}^M(\tau; \omega) \text{Im}g_{\mathbf{k}}(\tau; \omega), \quad (2.35)$$

$$\frac{1}{2}(\hat{\Sigma}^I\hat{g} + \hat{g}^\dagger\hat{\Sigma}^I)_{(\tau; \omega)} \approx \Sigma_{\mathbf{k}}^I(\tau; \omega) \text{Reg}_{\mathbf{k}}(\tau; \omega), \quad (2.36)$$

so that our kinetic equation (2.34) becomes

$$\begin{aligned} & \partial_\tau \text{Reg}_{\mathbf{k}}(\tau; \omega) + 2[\omega - \epsilon_{\mathbf{k}} - \Sigma_{\mathbf{k}}^M(\tau; \omega)] \text{Im}g_{\mathbf{k}}(\tau; \omega) \\ & = i\Sigma_{\mathbf{k}}^K(\tau; \omega) - \Sigma_{\mathbf{k}}^I(\tau; \omega) \text{Reg}_{\mathbf{k}}(\tau; \omega). \end{aligned} \quad (2.37)$$

Next, let us neglect the term involving the imaginary part of $g_{\mathbf{k}}(\tau; \omega)$ and set $\omega = \epsilon_{\mathbf{k}}$. Defining the quasi-particle distribution function $g_{\mathbf{k}}(\tau) = \text{Reg}_{\mathbf{k}}(\tau; \omega = \epsilon_{\mathbf{k}})$ we arrive at the simplified kinetic equation

$$\partial_\tau g_{\mathbf{k}}(\tau) = i\Sigma_{\mathbf{k}}^K(\tau; \epsilon_{\mathbf{k}}) - \Sigma_{\mathbf{k}}^I(\tau; \epsilon_{\mathbf{k}})g_{\mathbf{k}}(\tau). \quad (2.38)$$

Setting $g_{\mathbf{k}}(\tau) = 1 + 2n_{\mathbf{k}}(\tau)$, this equation can also be written as

$$\partial_\tau 2n_{\mathbf{k}}(\tau) = \Sigma_{\mathbf{k}}^{\text{in}}(\tau) - \Sigma_{\mathbf{k}}^{\text{out}}(\tau), \quad (2.39)$$

where the “in-scattering” and “out-scattering” self-energies are given by

$$\Sigma_{\mathbf{k}}^{\text{in}}(\tau) = i\Sigma_{\mathbf{k}}^K(\tau; \epsilon_{\mathbf{k}}), \quad (2.40a)$$

$$\Sigma_{\mathbf{k}}^{\text{out}}(\tau) = \Sigma_{\mathbf{k}}^I(\tau; \epsilon_{\mathbf{k}})[1 + 2n_{\mathbf{k}}(\tau)]. \quad (2.40b)$$

To make further progress, we need approximate expressions for the nonequilibrium self-energies $\Sigma_{\mathbf{k}}^K(\tau; \epsilon_{\mathbf{k}})$ and $\Sigma_{\mathbf{k}}^I(\tau; \epsilon_{\mathbf{k}})$. In Appendix B we give perturbative expressions for these self-energies to second order in the magnon-phonon coupling γ_q . Note that the simplest way to obtain the self-energies to this order is to perform a Hartree-Fock decoupling of the interaction term of the effective boson action (2.19). Within the same approximation as above (factorization of Wigner transforms, neglecting renormalization of the magnon energies, see Appendix C for details) we obtain

$$i\Sigma_{\mathbf{k}}^K(\tau; \epsilon_{\mathbf{k}}) = \frac{1}{V} \sum_{\mathbf{k}'} \{ [1 + n_{\mathbf{k}'}(\tau)] W_{\mathbf{k}', \mathbf{k}} + W_{\mathbf{k}, \mathbf{k}'} n_{\mathbf{k}'}(\tau) \}, \quad (2.41)$$

$$\Sigma_{\mathbf{k}}^I(\tau; \epsilon_{\mathbf{k}}) = \frac{1}{V} \sum_{\mathbf{k}'} \{ [1 + n_{\mathbf{k}'}(\tau)] W_{\mathbf{k}', \mathbf{k}} - W_{\mathbf{k}, \mathbf{k}'} n_{\mathbf{k}'}(\tau) \}, \quad (2.42)$$

where the transition rates $W_{\mathbf{k}, \mathbf{k}'}$ are given in Eq. (2.2). Substituting Eqs. (2.41, 2.42) into the kinetic equation (2.38) and renaming $\tau \rightarrow t$ we finally arrive at the rate equation (2.1).

For finite systems the δ -functions in the phonon spectral function (2.4) appearing in the perturbative expression (2.2) for the transition rates should be regularized. The simplest possibility is to perform an ad hoc replacement of the δ -functions by Lorentzians with finite width²⁰, but this procedure introduces an additional phenomenological parameter into the problem. Microscopically, the coupling of the phonons to the magnon system automatically generates such a broadening. We therefore introduce renormalized phonon propagators involving the phonon self-energies $\Pi_{\mathbf{q}}^X(\tau; \omega)$, where $X = R, A, K$. Defining the mean and the spectral combinations of the retarded and advanced phonon self-energies,

$$\hat{\Pi}^M = \frac{1}{2}[\hat{\Pi}^R + \hat{\Pi}^A], \quad \hat{\Pi}^I = i[\hat{\Pi}^R - \hat{\Pi}^A], \quad (2.43)$$

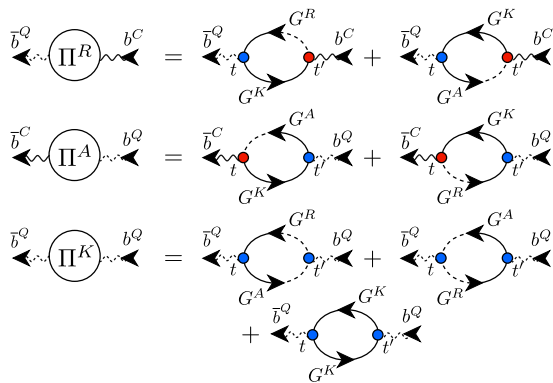


FIG. 3. (Color online) Diagrams representing the phonon self-energies Π^R , Π^A and Π^K to second order in the magnon-phonon interaction. Wavy lines represent the external phonon fields b^C and b^Q , while arrows represent the magnon Green functions G^R , G^A and G^K . We use the convention that the classical field components are represented by solid lines, while the quantum components are represented by dotted lines, see also the caption of Fig. 2. If we introduce in our FRG approach a hybridization cutoff only in the phonon propagators, these diagrams are finite at the initial cutoff scale.

the Wigner transforms of the renormalized phonon propagators can be written as

$$F_q^R(\tau; \omega) = \frac{1}{\omega - \omega_q - \Pi_q^R(\tau; \omega)}, \quad (2.44a)$$

$$F_q^A(\tau; \omega) = \frac{1}{\omega - \omega_q - \Pi_q^A(\tau; \omega)}, \quad (2.44b)$$

$$F_q^I(\tau; \omega) = \frac{\Pi_q^I(\tau; \omega)}{[\omega - \omega_q - \Pi_q^M(\tau; \omega)]^2 + [\frac{1}{2}\Pi_q^I(\tau; \omega)]^2}, \quad (2.44c)$$

$$iF_q^K(\tau; \omega) = \coth\left(\frac{\beta\omega}{2}\right) F_q^I(\tau; \omega). \quad (2.44d)$$

The diagrams of the phonon self-energies up to second order in the magnon-phonon coupling γ_q are shown in Fig. 3. Approximating the Wigner transforms as discussed above, and neglecting the real parts of the self-energies, we have $\Pi^M \approx 0$ and $\Pi^R \approx \frac{i}{2}\Pi^I \approx -\Pi^A$, where the spectral component of the phonon self-energy is

$$\begin{aligned} \Pi_q^I(\tau; \omega) &= \frac{2\pi}{V} \gamma_q^2 \sum_{\mathbf{k}} \delta(\omega + \epsilon_{\mathbf{k}-\mathbf{q}} - \epsilon_{\mathbf{k}}) \\ &\quad \times \{n_{\mathbf{k}-\mathbf{q}}(\tau) - n_{\mathbf{k}}(\tau)\}. \end{aligned} \quad (2.45)$$

To obtain regular results also for finite magnon gases, we evaluate the right-hand side of Eq. (2.45) in the limit of infinite volume, where $\Pi_q^I(\tau; \omega)$ is a continuous function

of all of its arguments. Let us emphasize that we take the limit $V \rightarrow \infty$ only in the phonon self-energies, so that with the resulting regular transition rates we can still use our rate equation (2.1) to describe the kinetics of a finite magnon system with discrete spectrum.

III. FUNCTIONAL RENORMALIZATION GROUP APPROACH

Formally exact FRG flow equations for the irreducible vertices of any bosonic many-body systems out of equilibrium^{16,17} can be obtained as a special case of the general hierarchy of FRG flow equations¹³ which follows from the Wetterich equation³⁵. While it is straightforward to write down these equations, the proper identification of a sensible cutoff procedure which does not violate causality and respects the fluctuation-dissipation theorem under equilibrium conditions is rather delicate problem. It turns out that for the coupled magnon-phonon system considered here a modified hybridization cutoff scheme^{17,36} is most convenient. In this scheme the infinitesimal imaginary parts $\pm i\eta$ defining the boundary conditions of the retarded and advanced propagators are replaced by finite quantities $\pm i\Lambda$, where Λ is identified with the flow-parameter of the renormalization group procedure. Moreover, in the hybridization cutoff scheme the same replacement is also made in the Keldysh blocks of the inverse Gaussian propagators, see Eqs. (2.17a) and (2.17b). For bosonic systems, however, one should be careful to take into account that the spectral function should be positive for positive frequencies, and negative for negative frequencies²⁸. The imaginary part of the spectral component of the self-energy therefore changes sign at zero frequency. Hence, in the bosonic version of the hybridization cutoff scheme the infinitesimal imaginary part η should be replaced by $\eta \rightarrow \Lambda \text{sgn}(\omega)$. In contrast, for fermions the spectral function is positive for all frequencies, so that the hybridization cutoff should be introduced by replacing $\eta \rightarrow \Lambda$.

In this work, we introduce a hybridization cutoff *only in the phonon propagators*, while keeping the $\pm i\eta$ in the magnon propagators infinitesimal. In this way we do not artificially smear out the magnon distribution, so that we can still describe the nonequilibrium dynamics in terms of a kinetic equation describing the evolution of the occupation probabilities of sharp energy levels. The cutoff-dependent Keldysh action $S_\Lambda[\bar{a}, a, \bar{b}, b]$ with a hybridization cutoff in the phonon propagators can be obtained from the action $S[\bar{a}, a, \bar{b}, b]$ given in Eq. (2.15) by replacing the Gaussian phonon propagators by cutoff-dependent propagators,

$$\begin{aligned}
S_\Lambda[\bar{a}, a, \bar{b}, b] = & \int dt \int dt' \left\{ \sum_{\mathbf{k}} (\bar{a}_{\mathbf{k}}^C(t), \bar{a}_{\mathbf{k}}^Q(t)) \begin{pmatrix} 0 & (\hat{G}_0^A)^{-1} \\ (\hat{G}_0^R)^{-1} & 2i\eta\hat{g}_0 \end{pmatrix}_{tt'} \begin{pmatrix} a_{\mathbf{k}}^C(t') \\ a_{\mathbf{k}}^Q(t') \end{pmatrix} \right. \\
& + \left. \sum_{\mathbf{q}} (\bar{b}_{\mathbf{q}}^C(t), \bar{b}_{\mathbf{q}}^Q(t)) \begin{pmatrix} 0 & (\hat{F}_\Lambda^A)^{-1} \\ (\hat{F}_\Lambda^R)^{-1} & -(\hat{F}_\Lambda^R)^{-1}\hat{F}_\Lambda^K(\hat{F}_\Lambda^A)^{-1} \end{pmatrix}_{tt'} \begin{pmatrix} b_{\mathbf{q}}^C(t') \\ b_{\mathbf{q}}^Q(t') \end{pmatrix} \right\} \\
& - \int dt \frac{1}{\sqrt{V}} \sum_{\mathbf{k}, \mathbf{q}} \gamma_{\mathbf{q}} \left[(\bar{a}_{\mathbf{k}+\mathbf{q}}^C a_{\mathbf{k}}^Q + \bar{a}_{\mathbf{k}+\mathbf{q}}^Q a_{\mathbf{k}}^C) X_{\mathbf{q}}^C + (\bar{a}_{\mathbf{k}+\mathbf{q}}^C a_{\mathbf{k}}^C + \bar{a}_{\mathbf{k}+\mathbf{q}}^Q a_{\mathbf{k}}^Q) X_{\mathbf{q}}^Q \right]. \quad (3.1)
\end{aligned}$$

Because for $\Lambda \rightarrow \infty$ all phonon propagators vanish, the FRG flow should be integrated with the boundary condition that all irreducible pure magnon vertices vanish for $\Lambda \rightarrow \infty$. This implies that all closed loops involving only magnon propagators do not vanish in this limit, leading to a non-trivial initial condition for the FRG flow. This is analogous to the bosonic momentum transfer cutoff scheme^{13,37} in coupled fermion-boson systems, where at the initial scale all pure boson vertices are finite. In particular, in the present problem the phonon self-energy diagrams shown in Fig. 3 are finite at the initial scale. Neglecting the renormalization of the real part of the phonon self-energies, the scale-dependent phonon propagators are in our cutoff scheme given by

$$F_{\Lambda, \mathbf{q}}^R(\tau; \omega) = \frac{1}{\omega - \omega_{\mathbf{q}} + i\Lambda \text{sgn}\omega + \frac{i}{2}\Pi_{\Lambda, \mathbf{q}}^I(\tau; \omega)}, \quad (3.2a)$$

$$F_{\Lambda, \mathbf{q}}^A(\tau; \omega) = \frac{1}{\omega - \omega_{\mathbf{q}} - i\Lambda \text{sgn}\omega - \frac{i}{2}\Pi_{\Lambda, \mathbf{q}}^I(\tau; \omega)}, \quad (3.2b)$$

$$F_{\Lambda, \mathbf{q}}^I(\tau; \omega) = \frac{2\Lambda \text{sgn}\omega + \Pi_{\Lambda, \mathbf{q}}^I(\tau; \omega)}{(\omega - \omega_{\mathbf{q}})^2 + [\Lambda \text{sgn}\omega + \frac{1}{2}\Pi_{\Lambda, \mathbf{q}}^I(\tau; \omega)]^2}, \quad (3.2c)$$

$$iF_{\Lambda, \mathbf{q}}^K(\tau; \omega) = \coth\left(\frac{\beta\omega}{2}\right) F_{\Lambda, \mathbf{q}}^I(\tau; \omega), \quad (3.2d)$$

where the imaginary part of the scale-dependent phonon self-energy is approximated by an expression similar to Eq. (2.45),

$$\begin{aligned}
\Pi_{\Lambda, \mathbf{q}}^I(\tau; \omega) = & \frac{2\pi}{V} \gamma_{\mathbf{q}}^2 \sum_{\mathbf{k}} \delta(\omega + \epsilon_{\mathbf{k}-\mathbf{q}} - \epsilon_{\mathbf{k}}) \\
& \times \{n_{\Lambda, \mathbf{k}-\mathbf{q}}(\tau) - n_{\Lambda, \mathbf{k}}(\tau)\}, \quad (3.3)
\end{aligned}$$

where $n_{\Lambda, \mathbf{k}}(\tau)$ is the scale-dependent magnon distribution function, and it is understood that for our numerical calculations we replace $V^{-1} \sum_{\mathbf{k}} \rightarrow \int d^2k / (2\pi)^2$ to obtain a smooth phonon self-energy in our two-dimensional system. Note that the scale parameter Λ can be considered as an additional contribution to the imaginary part of the phonon self-energy, which arises from the hybridization between phonons and magnons. Introducing the hybridization function

$$\Lambda_{\mathbf{q}}(\tau; \omega) \equiv \Lambda \text{sgn}\omega + \frac{1}{2}\Pi_{\Lambda, \mathbf{q}}^I(\tau; \omega), \quad (3.4)$$

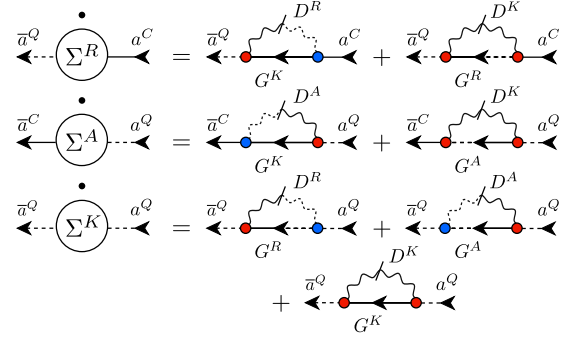


FIG. 4. (Color online) Graphical representation of the truncated FRG flow equations for the nonequilibrium magnon self-energies with hybridization cutoff in the phonon propagators. The dots over the self-energy symbols on the left-hand side represent the derivative with respect to the cutoff parameter Λ . Slashed wavy lines on the right-hand side represent single-scale phonon propagators, which can be obtained by taking the partial derivative of Eqs. (3.5a–3.5d) with respect to the explicit Λ -dependence. Note that the diagrams on the right-hand side can be obtained from the self-energy diagrams given in Appendix B (see Fig. 6) by simply replacing the phonon-propagators by the corresponding single-scale propagators.

the symmetrized phonon propagators can be written as

$$D_{\Lambda, \mathbf{q}}^R(\omega) = \frac{\omega_{\mathbf{q}} - i\Lambda_{\mathbf{q}}(\tau; \omega)}{\omega^2 - [\omega_{\mathbf{q}} - i\Lambda_{\mathbf{q}}(\tau; \omega)]^2}, \quad (3.5a)$$

$$D_{\Lambda, \mathbf{q}}^A(\omega) = \frac{\omega_{\mathbf{q}} + i\Lambda_{\mathbf{q}}(\tau; \omega)}{\omega^2 - [\omega_{\mathbf{q}} + i\Lambda_{\mathbf{q}}(\tau; \omega)]^2}, \quad (3.5b)$$

$$\begin{aligned}
D_{\Lambda, \mathbf{q}}^I(\omega) = & \frac{\Lambda_{\mathbf{q}}(\tau; \omega)}{(\omega - \omega_{\mathbf{q}})^2 + \Lambda_{\mathbf{q}}^2(\tau; \omega)} \\
& + \frac{\Lambda_{\mathbf{q}}(\tau; \omega)}{(\omega + \omega_{\mathbf{q}})^2 + \Lambda_{\mathbf{q}}^2(\tau; \omega)}, \quad (3.5c)
\end{aligned}$$

$$iD_{\Lambda, \mathbf{q}}^K(\omega) = \coth\left(\frac{\beta\omega}{2}\right) D_{\Lambda, \mathbf{q}}^I(\omega). \quad (3.5d)$$

The general form of nonequilibrium FRG flow equations for interacting bosons in the Keldysh basis has been written down in Refs. [16 and 17]. Here we use a simple truncation where the renormalization of the magnon-phonon vertex is neglected. The relevant FRG flow equations for the nonequilibrium magnon self-energies with hybridization cutoff in the phonon propagators are shown graphically in Fig. 4. For the explicit evaluation of these expressions, we use the same approximations as in the

derivation of the perturbative rate equation (2.1) outlined in Sec. II, namely:

1. Keep only the leading terms in the gradient expansion so that Wigner transforms of products of infinite matrices in the time labels factorize.
2. Neglect the contributions in the kinetic equation describing the renormalization of the magnon energies.
3. Take the frequency argument of the self-energies on resonance, $\omega = \epsilon_{\mathbf{k}}$.

After straightforward manipulations analogous to those described in Sec. II we obtain a system of three coupled partial differential equations for the scale-dependent magnon distribution function $n_{\Lambda, \mathbf{k}}(\tau)$ and the scale-dependent nonequilibrium self-energies $\Sigma_{\Lambda, \mathbf{k}}^K(\tau; \epsilon_{\mathbf{k}})$ and $\Sigma_{\Lambda, \mathbf{k}}^I(\tau; \epsilon_{\mathbf{k}})$. The FRG version of the kinetic equation is formally identical with the perturbative kinetic equation (2.38),

$$\partial_\tau 2n_{\Lambda, \mathbf{k}}(\tau) = i\Sigma_{\Lambda, \mathbf{k}}^K(\tau; \epsilon_{\mathbf{k}}) - \Sigma_{\Lambda, \mathbf{k}}^I(\tau; \epsilon_{\mathbf{k}}) [1 + 2n_{\Lambda, \mathbf{k}}(\tau)]. \quad (3.6)$$

In contrast to the perturbative equation (2.38) where the nonequilibrium self-energies can be expressed as integrals depending on the distribution function [see Eqs. (2.41, 2.42)], in our FRG approach the self-energies are determined by flow equations relating their derivatives with respect to the cutoff Λ to the Λ -dependent distribution function,

$$\partial_\Lambda i\Sigma_{\Lambda, \mathbf{k}}^K(\tau; \epsilon_{\mathbf{k}}) = \frac{1}{V} \sum_{\mathbf{k}'} \{ [1 + n_{\Lambda, \mathbf{k}'}(\tau)] \dot{W}_{\mathbf{k}', \mathbf{k}} + \dot{W}_{\mathbf{k}, \mathbf{k}'} n_{\Lambda, \mathbf{k}'}(\tau) \}, \quad (3.7)$$

$$\partial_\Lambda \Sigma_{\Lambda, \mathbf{k}}^I(\tau; \epsilon_{\mathbf{k}}) = \frac{1}{V} \sum_{\mathbf{k}'} \{ [1 + n_{\Lambda, \mathbf{k}'}(\tau)] \dot{W}_{\mathbf{k}', \mathbf{k}} - \dot{W}_{\mathbf{k}, \mathbf{k}'} n_{\Lambda, \mathbf{k}'}(\tau) \}. \quad (3.8)$$

Here $\dot{W}_{\mathbf{k}, \mathbf{k}'}$ is the partial derivative of the cutoff-dependent transition rate with respect to the explicit Λ -dependence,

$$\dot{W}_{\mathbf{k}, \mathbf{k}'} = 2\gamma_{\mathbf{k}-\mathbf{k}'}^2 \dot{D}_{\Lambda, \mathbf{k}-\mathbf{k}'}^I(\epsilon_{\mathbf{k}} - \epsilon_{\mathbf{k}'}) b(\epsilon_{\mathbf{k}} - \epsilon_{\mathbf{k}'}), \quad (3.9)$$

which has the same structure as Eq. (2.2), but with the phonon spectral function $D_{\Lambda, \mathbf{q}}^I(\omega)$ replaced by

$$\dot{D}_{\Lambda, \mathbf{q}}^I(\omega) = \pi \text{sgn} \omega [L'_{\Lambda, \mathbf{q}}(\tau; \omega)(\omega - \omega_{\mathbf{q}}) + L'_{\Lambda, \mathbf{q}}(\tau; \omega)(\omega + \omega_{\mathbf{q}})], \quad (3.10)$$

where

$$L'_\Lambda(\omega) = \partial_\Lambda \left[\frac{1}{\pi} \frac{\Lambda}{\omega^2 + \Lambda^2} \right] = \frac{1}{\pi} \frac{\omega^2 - \Lambda^2}{(\omega^2 + \Lambda^2)^2} \quad (3.11)$$

is the derivative of a normalized Lorentzian with respect to its width. Note that the right-hand side of Eq. (3.10) implicitly depends on the time τ via the τ -dependence of

the phonon self-energy $\Pi_{\Lambda, \mathbf{q}}^I(\tau; \omega)$ given in Eq. (2.45). To simplify the numerical evaluation of the above system of integro-differential equations, we shall replace in Sec. IV the phonon self-energy by its equilibrium value at vanishing cutoff, which is approached for $\tau \rightarrow \infty$. In other words, we replace

$$\Pi_{\Lambda, \mathbf{q}}^I(\tau; \omega) \rightarrow \Pi_{\Lambda=0, \mathbf{q}}^I(\tau = \infty; \omega). \quad (3.12)$$

This procedure can be justified by noting that for sufficiently large values of the cutoff parameter Λ the contribution from the phonon self-energy to the hybridization function $\Lambda_{\mathbf{q}}(\tau; \omega)$ defined in Eq. (3.4) can be neglected, so that the only for small Λ the effect of the phonon self-energy becomes important; but in this regime the magnon distribution is already close to its equilibrium value.

Unfortunately, the above system of equations violates particle number conservation, in contrast to the perturbative kinetic equation (2.1), which obviously implies

$$\frac{\partial}{\partial t} \sum_{\mathbf{k}} n_{\mathbf{k}}(t) = 0. \quad (3.13)$$

The fact that Eqs. (3.6–3.8) violate particle number conservation is related to our approximation of neglecting the renormalization of the real part of the magnon energies. Note that particle number conservation is related to the $U(1)$ -symmetry of the bare action $S_\Lambda[\bar{a}, a, \bar{b}, b]$ given in Eq. (3.1). To see this more clearly, let us multiply the magnon fields in Eq. (3.1) by an arbitrary scale- and time-dependent phase factor ($X = C, Q$),

$$a_{\mathbf{k}}^X(t) = e^{i\alpha_\Lambda(t)} a_{\mathbf{k}}^{\prime X}(t), \quad \bar{a}_{\mathbf{k}}^X(t) = e^{-i\alpha_\Lambda(t)} \bar{a}_{\mathbf{k}}^{\prime X}(t). \quad (3.14)$$

Then the Keldysh action (3.1) changes as follows,

$$S_\Lambda[e^{-i\alpha} \bar{a}', e^{i\alpha} a', \bar{b}, b] = S_\Lambda[\bar{a}', a', \bar{b}, b] - \int dt \frac{d\alpha_\Lambda(t)}{dt} \sum_{\mathbf{k}} \left[\bar{a}_{\mathbf{k}}^{\prime C}(t) a_{\mathbf{k}}^{\prime Q}(t) + \bar{a}_{\mathbf{k}}^{\prime Q}(t) a_{\mathbf{k}}^{\prime C}(t) \right]. \quad (3.15)$$

The additional term can be absorbed via a shift in the retarded and advanced self-energies,

$$[\hat{\Sigma}^R]_{tt'} \rightarrow [\hat{\Sigma}^R]_{tt'} + \delta(t-t') \frac{d\alpha_\Lambda(t)}{dt}, \quad (3.16a)$$

$$[\hat{\Sigma}^A]_{tt'} \rightarrow [\hat{\Sigma}^A]_{tt'} + \delta(t-t') \frac{d\alpha_\Lambda(t)}{dt}. \quad (3.16b)$$

The extra terms drop out in the spectral self-energy $\hat{\Sigma}^I = i[\hat{\Sigma}^R - \hat{\Sigma}^A]$, but survive in the average $\hat{\Sigma}^M = \frac{1}{2}[\hat{\Sigma}^R + \hat{\Sigma}^A]$. By completely neglecting the symmetric combination $\hat{\Sigma}^M$ in our derivation of Eq. (3.6), we have lost the possibility of explicitly implementing the condition of particle number conservation. To impose the constraint of constant particle number on the FRG flow, we add the corresponding symmetric self-energy $\hat{\Sigma}^M$ to the left-hand side of the kinetic equation. For our purpose, it is sufficient to approximate

$$[\hat{\Sigma}^M]_{tt'} = -\delta(t-t') \mu_\Lambda(t). \quad (3.17)$$

The only effect of $\mu_\Lambda(t)$ on the kinetic equation (3.6) is to replace the derivative ∂_τ by the corresponding covariant derivative $\partial_\tau + \mu_\Lambda(\tau)$. Note that the time-dependent Lagrange multiplier $\mu_\Lambda(\tau)$ enforcing the constraint of particle-number conservation appears in the quantum dynamics as a gauge-field³⁸. As a result, Eq. (3.6) should be replaced by

$$[\partial_\tau + \mu_\Lambda(\tau)]2n_{\Lambda,\mathbf{k}}(\tau) = i\Sigma_{\Lambda,\mathbf{k}}^K(\tau; \epsilon_{\mathbf{k}}) - \Sigma_{\Lambda,\mathbf{k}}^I(\tau; \epsilon_{\mathbf{k}}) [1 + 2n_{\Lambda,\mathbf{k}}(\tau)]. \quad (3.18)$$

The energy $\mu_\Lambda(\tau)$ plays the role of a scale- and time-dependent Lagrange multiplier, which should be adjusted such that the total particle number $N = \sum_{\mathbf{k}} n_{\Lambda,\mathbf{k}}(\tau)$ is conserved for all times τ and for all values of the cutoff Λ , implying

$$\partial_\tau N = \sum_{\mathbf{k}} \partial_\tau n_{\Lambda,\mathbf{k}}(\tau) = 0. \quad (3.19)$$

Substituting Eq. (3.18) into the right-hand side of this equation, we conclude that the scale- and time dependent Lagrange multiplier is explicitly given by

$$\mu_\Lambda(\tau) = \frac{1}{2N} \sum_{\mathbf{k}} \left\{ i\Sigma_{\Lambda,\mathbf{k}}^K(\tau; \epsilon_{\mathbf{k}}) - \Sigma_{\Lambda,\mathbf{k}}^I(\tau; \epsilon_{\mathbf{k}}) [1 + 2n_{\Lambda,\mathbf{k}}(\tau)] \right\}. \quad (3.20)$$

Combining Eqs. (3.18) and (3.20) with Eqs. (3.7), (3.8) and (2.45) we obtain a closed system of particle-number conserving FRG flow equations which can be used to calculate the nonequilibrium time evolution of the magnon distribution function. In the following section we shall use these equations to calculate the thermalization of the magnon gas in YIG.

To conclude this section, let us summarize and justify our main approximations. First of all, we have retained only the leading terms in the gradient expansion, which amounts to the factorization of Wigner transforms. This procedure is justified if all functions vary sufficiently slowly in space and time. For YIG this approximation seems to be well justified, because an alternative description in terms of the phenomenological Landau-Lifshitz equation (which rely on similar assumptions) has been highly successful²⁵. Moreover, we have set the energy argument of all functions on resonance. Also this approximation is justified for YIG, because experimentally magnons in YIG are known to behave as well-defined quasiparticles. Finally, we have neglected the renormalization of the magnon energies. By fitting the magnon dispersion in our final expressions to experimental data, we implicitly take this effect into account.

IV. THERMALIZATION OF MAGNONS IN YIG

Quantized spin-waves (magnons) in ordered magnets obey to a very good approximation Bose statistics, so

that magnetic insulators can serve as relatively easily accessible model systems for investigating the nonequilibrium dynamics of bosons. A particularly well characterized magnet is yttrium-iron garnet (YIG)²¹. The momentum distribution function of the magnon gas in YIG has been probed experimentally using the technique of Brillouin light scattering^{6,22,23,39}.

At long wavelengths the energy dispersion of the experimentally relevant magnon band in thin YIG-stripes can be approximated by Eq. (1.2). The values of the exchange stiffness ρ_{ex} and the dipolar energy scale Δ entering Eq. (1.2) can be written as $\rho_{\text{ex}} = JSa^2$ and $\Delta = 4\pi\mu M_s$, where $J \approx 1.29$ K is the nearest neighbor exchange constant of YIG and the saturation magnetization is given by $4\pi M_s \approx 1750$ G. Here $a \approx 12.376$ Å is the lattice constant and $\mu = g\mu_B$ is the magnetic moment of the localized spins²⁴. If we arbitrarily set the effective g -factor equal to two so that $\mu = 2\mu_B$, then the effective spin is $S = M_s a^3 / \mu \approx 14.2$. Due to an interplay between exchange interactions, dipole-dipole interactions, and finite-size effects, the magnon dispersion of YIG exhibits two degenerate minima at finite momenta $\pm k_{\text{min}} \hat{z}$, where \hat{z} is the direction of the external magnetic field. Having fixed the energy dispersion, the only adjustable parameters of our model Hamiltonian (1.1) are the phonon velocity $c = \omega_{\mathbf{q}} / |\mathbf{q}|$ and the magnon-phonon coupling constant $\gamma = \gamma_{\mathbf{q}} / \sqrt{|\mathbf{q}|}$.

Highly excited nonequilibrium states of the magnon gas in YIG can be generated via parametric pumping with a time-dependent external microwave source. Once the microwave source has been switched off, the thermalization of the magnon gas can be directly observed^{22,23}. In particular, in Ref. [23] the time evolution of the momentum distribution function $n_{\mathbf{k}}(t)$ of the magnon gas in YIG has been measured. The data presented by Demidov *et al.*²³ show how a highly excited initial state evolves towards a thermal equilibrium state where the occupation of the magnon modes at the bottom of the spectrum is strongly enhanced. Whether or not such a state should be called a Bose-Einstein condensate of magnons seems to be a matter of semantics^{40,41}. We have argued previously^{26,42} that the experimentally observed strong enhancement of the magnon distribution is not accompanied by superfluidity, because a macroscopic occupation of a certain magnon mode is simply equivalent with a change in magnetic order⁴³.

In Fig. 5 we show our results for the time evolution of the magnon distribution obtained from the numerical solution of the FRG rate equations (3.7, 3.8) and the particle number conserving kinetic equation given in Eqs. (3.18, 3.20). For the numerical calculations we have used the energy dispersion (1.2) with experimentally relevant parameters discussed above and stripe thickness $d = 5 \mu\text{m}$. The minima of the dispersion are located at $|k_{\parallel}| = 5.5 \times 10^4 \text{ cm}^{-1} \equiv k_{\text{min}}$ and $k_{\perp} = 0$. For simplicity we consider a square stripe with the length of $L = 4.58 \mu\text{m}$ and work with a truncated momentum space such that $|k_{\parallel}| \leq 41.1 \times 10^4 \text{ cm}^{-1}$

and $|k_{\perp}| \leq 13.7 \times 10^4 \text{ cm}^{-1}$, corresponding to 61×21 points in momentum space. The rate equation and the flow equations are solved simultaneously as described in Ref. [17]. In order to calculate the imaginary part of the phonon self-energy as discussed in Secs. II and III we have used a two-dimensional adaption of the tetrahedron method⁴⁴. The initial cutoff Λ_0 was chosen to be $404\Omega_0$, where $\Omega_0 = ck_{\text{min}}$ is the relevant energy scale for the phonon dynamics. We have set the phonon velocity in YIG to $c = 7.15 \times 10^5 \text{ cm/s}$ as measured in Ref. [45]. For the numerical calculations we have divided the time interval into 3240 equidistant steps up to a final time of 670 ns. For small values of the flow parameter $\Lambda \lesssim \Omega_0$ the dependence of the magnon self-energies on Λ is rather strong. We have therefore divided the range of Λ into two intervals, $[0, 4\Omega_0]$ and $[4\Omega_0, \Lambda_0]$, each equidistantly discretized with 500 points. Our theoretical results shown in Fig. 5 agree quite well with the corresponding experimental data shown in Fig. 3 of Ref. [23]. Note that in our simple model the order parameter $\langle a_{\mathbf{k}}^C(t) \rangle$ vanishes, so that the global $U(1)$ symmetry of the Hamiltonian (1.1) is not spontaneously broken and our magnon gas is not superfluid. Nevertheless, our model describes the experimentally observed thermalization towards a magnon state with strongly enhanced occupation at the bottom of the spectrum, indicating that the experiments observing BEC of magnons in YIG can be explained without postulating that the magnon state is superfluid.

Of course, the thermalization of the magnon gas in YIG is not exclusively driven by magnon-phonon interactions, but also by many-body scattering processes involving two or more magnons. In particular, interactions involving three and four powers of the magnon operators should be added to obtain a more realistic model for the magnon gas in YIG²⁶. While the three-magnon vertices yield the dominant contribution to the magnon damping⁴⁶, the four-magnon vertices compete with the magnon-phonon interaction to re-distribute the excited initial state over the magnon spectrum. The inclusion of these scattering processes into our FRG formalism is in principle possible but requires substantial extensions of the present formalism which are beyond the scope of this work. On the other hand, experiments show that magnons in YIG behave as well-defined, weakly interacting quasiparticles, even in an external microwave field. Our assumption that the initial state at $t = 0$ is not correlated is therefore well justified for YIG.

Finally, let us point out that the magnon-phonon interaction in our model Hamiltonian (1.1) conserves the number of magnons because the phonon field $X_{\mathbf{q}}$ couples only to the magnon density $\hat{\rho}_{\mathbf{q}}$. However, we expect that in YIG there should exist another type of magnon-phonon interaction involving the combinations $a_{\mathbf{k}}^{\dagger} a_{-\mathbf{k}-\mathbf{q}}^{\dagger} X_{\mathbf{q}}$ and $a_{-\mathbf{k}} a_{\mathbf{k}+\mathbf{q}} X_{-\mathbf{q}}$. This type of magnon-phonon coupling does not conserve the magnon number and leads to an efficient energy transfer from the magnons into the phonon system. Microscopically, this magnon-phonon interaction arises from the fact that the quasi-particle operators $a_{\mathbf{k}}$

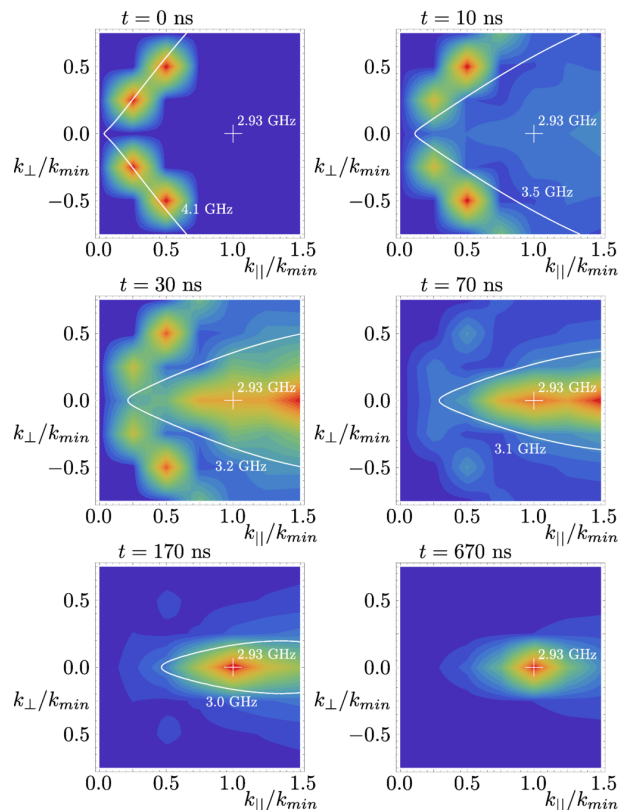


FIG. 5. (Color online) These contour plots show an interpolation of the magnon distribution of YIG on a 7×7 -mesh in momentum space for different times. The white contour lines denote the magnon spectrum of YIG for fixed energies. The crosses mark the minimum of the dispersion. The results are presented such that they are directly comparable with the experimental data of Ref. [23]. We have shifted the zero of time to the moment where the microwave pumping is switched off. For the calculation of the dispersion of YIG we have used the parameters from Ref. [24], which differ slightly from the parameters used in Ref. [23]. The initial state is chosen such that magnons with an energy of 4.1 GHz in the area $|k_{\perp}| < 0.5k_{\text{min}}$ are equally occupied, which resembles the initial magnon distribution in the experiment after the pumping has been switched off. The strength of the magnon-phonon interaction has been adjusted such that the occupation of the ground state is saturated after approximately 670 ns, which gives $\gamma = 2.0 \times 10^{-7} \text{ cm}\sqrt{\text{GHz}}$. Finally, we have used typical experimental values for temperature ($T = 300 \text{ K}$), magnetic field ($H = 1000 \text{ Oe}$), and magnon density ($4.77 \times 10^6 / \mu\text{m}^2$).

describing the physical magnon excitations of YIG are related via a canonical (Bogoliubov) transformation to the Holstein-Primakoff bosons resulting from the bosonization of the spin operators; see Ref. [47] for a microscopic derivation of these terms for a frustrated antiferromagnet. Even if the couplings of these processes in YIG are small, we expect that these processes are important to describe the experimentally observed⁷ long-time decay of the BEC.

V. CONCLUSIONS

In summary, we have studied the thermalization of the magnon gas due to coupling to the thermal phonon bath in thin films of the magnetic insulator yttrium-iron garnet. Although we have only retained the interaction processes which conserve the total number of magnons, our theoretical predictions for the time evolution of the momentum distribution of the magnons agrees quite well with experimental results. In particular, the accumulation of magnons at the bottom of the spectrum is correctly described within our approach.

We have intentionally considered in this work only the case where all nonequilibrium averages $\langle a_{\mathbf{k}}^C(t) \rangle$ vanish identically⁴⁸. These averages play the role of order parameters; keeping in mind that the magnon operators in YIG describe the quantized fluctuations around the classical ground states, macroscopic values of $\langle a_{\mathbf{k}}^C(t) \rangle$ for one or several wave-vectors describe a macroscopic reorganization of the magnetic state⁴². To describe this phenomenon microscopically, it is necessary to take the magnon-magnon interactions into account.

The present work describes also some technical advance: we have developed an implementation of the nonequilibrium functional renormalization group method which clearly exhibits the connection to a conventional rate equation approach. In a sense, our FRG approach can be considered as a simple renormalization group extension of a rate equation approach. The main advantages of our approach are that our FRG resummation goes beyond the simple second order approximation for the collision terms in the kinetic equation, and that our method allows us to include in a simple way the feedback of the magnon dynamics on the phonon propagators which in turn determine the transition rates between the magnon states in the rate equation. We have also developed a generalized hybridization cutoff scheme for interacting bosons. It is possible to generalize our approach to include magnon-magnon interactions or magnon number violating magnon-phonon interactions.

ACKNOWLEDGMENTS

We thank Mathieu Taillefumier for his help with the numerical calculations, and Sasha Chernyshev for sending us his recent preprint on magnon damping in YIG prior to publication. We also thank Andreas Kreisel and Oleksandr Serha for helpful discussions. Financial support by SFB/TRR49, the CNRS, and the Humboldt foundation is gratefully acknowledged.

APPENDIX A: QUANTUM KINETIC EQUATIONS

In this appendix we review several possibilities of writing down quantum kinetic equations. Although in the

main text we only make use of the Wigner transformed kinetic equation for the distribution function $g_{\mathbf{k}}(\tau; \omega)$ defined via Eq. (2.26), it is instructive to work out the precise relation between our parametrization and a formulation of the nonequilibrium problem in terms of the two-time Keldysh Green function.

1. Two-time Keldysh Green function

Writing the nonequilibrium Dyson equation (2.23) as

$$(\mathbf{G}_0^{-1} - \Sigma) \mathbf{G} = \mathbf{I} \quad (\text{A1})$$

we obtain following three equations for the sub-blocks,

$$(\hat{G}_0^R)^{-1} \hat{G}^R = \hat{I} + \hat{\Sigma}^R \hat{G}^R, \quad (\text{A2a})$$

$$(\hat{G}_0^A)^{-1} \hat{G}^A = \hat{I} + \hat{\Sigma}^A \hat{G}^A, \quad (\text{A2b})$$

$$(\hat{G}_0^R)^{-1} \hat{G}^K = \hat{\Sigma}^K \hat{G}^A + \hat{\Sigma}^R \hat{G}^K, \quad (\text{A2c})$$

where \hat{I} is the unit matrix in the momentum- and time labels. Alternatively we can also consider the corresponding ‘‘right Dyson equation’’,

$$\mathbf{G} (\mathbf{G}_0^{-1} - \Sigma) = \mathbf{I}, \quad (\text{A3})$$

which implies the following relations,

$$\hat{G}^R (\hat{G}_0^R)^{-1} = \hat{I} + \hat{G}^R \hat{\Sigma}^R, \quad (\text{A4a})$$

$$\hat{G}^A (\hat{G}_0^A)^{-1} = \hat{I} + \hat{G}^A \hat{\Sigma}^A, \quad (\text{A4b})$$

$$\hat{G}^K (\hat{G}_0^A)^{-1} = \hat{G}^R \hat{\Sigma}^K + \hat{G}^K \hat{\Sigma}^A. \quad (\text{A4c})$$

Subtracting the Keldysh component of the left and right-hand sides of the Dyson equations (A2c, A4c), we obtain the kinetic equation

$$[\hat{M}_0, \hat{G}^K] = \hat{\Sigma}^R \hat{G}^K - \hat{G}^R \hat{\Sigma}^K + \hat{\Sigma}^K \hat{G}^A - \hat{G}^K \hat{\Sigma}^A, \quad (\text{A5})$$

where $[\ , \]$ denotes the commutator, and \hat{M}_0 is defined in Eq. (2.31). Note that

$$(\hat{G}_0^R)^{-1} = \hat{M}_0 + i\eta \hat{I} \quad , \quad (\hat{G}_0^A)^{-1} = \hat{M}_0 - i\eta \hat{I}, \quad (\text{A6})$$

and

$$[\hat{M}_0 \hat{G}^K]_{tt'} = (i\partial_t - \epsilon_{\mathbf{k}}) G^K(t, t'), \quad (\text{A7a})$$

$$[\hat{G}^K \hat{M}_0]_{tt'} = (-i\partial_{t'} - \epsilon_{\mathbf{k}}) G^K(t, t'), \quad (\text{A7b})$$

implying

$$[\hat{M}_0, \hat{G}^K]_{tt'} = (i\partial_t + i\partial_{t'}) G^K(t, t'). \quad (\text{A8})$$

We conclude that in the time domain the quantum kinetic equation (A5) assumes the form

$$\begin{aligned} & (i\partial_t + i\partial_{t'})G^K(t, t') \\ &= \int_{t_0}^t dt_1 [\Sigma^R(t, t_1)G^K(t_1, t') - G^R(t, t_1)\Sigma^K(t_1, t')] \\ &+ \int_{t_0}^{t'} dt_1 [\Sigma^K(t, t_1)G^A(t_1, t') - G^K(t, t_1)\Sigma^A(t_1, t')]. \end{aligned} \quad (\text{A9})$$

To identify the operators which reduce in the appropriate limit to the collision integral in the Boltzmann equation, it is convenient to introduce³⁴ $\hat{\Sigma}^M = \frac{1}{2}[\hat{\Sigma}^R + \hat{\Sigma}^A]$ and $\hat{\Sigma}^I = i[\hat{\Sigma}^R - \hat{\Sigma}^A]$, see Eq. (2.32). The inverse relations are

$$\hat{\Sigma}^R = \hat{\Sigma}^M - \frac{i}{2}\hat{\Sigma}^I, \quad \hat{\Sigma}^A = \hat{\Sigma}^M + \frac{i}{2}\hat{\Sigma}^I. \quad (\text{A10})$$

A similar decomposition is also introduced for the retarded and advanced Green functions,

$$\hat{G}^M = \frac{1}{2}[\hat{G}^R + \hat{G}^A], \quad \hat{G}^I = i[\hat{G}^R - \hat{G}^A], \quad (\text{A11})$$

so that

$$\hat{G}^R = \hat{G}^M - \frac{i}{2}\hat{G}^I, \quad \hat{G}^A = \hat{G}^M + \frac{i}{2}\hat{G}^I. \quad (\text{A12})$$

Defining $\hat{M} = \hat{M}_0 - \hat{\Sigma}^M$ [see Eq. (2.28)], we may write the kinetic equation (A5) as

$$[\hat{M}, \hat{G}^K] - [\hat{\Sigma}^K, \hat{G}^M] = \hat{C}^{\text{in}} - \hat{C}^{\text{out}}, \quad (\text{A13})$$

where we have introduced the collision matrices

$$\hat{C}^{\text{in}} = \frac{i}{2}\{\hat{\Sigma}^K, \hat{G}^I\}, \quad (\text{A14})$$

$$\hat{C}^{\text{out}} = \frac{i}{2}\{\hat{\Sigma}^I, \hat{G}^K\}. \quad (\text{A15})$$

Recall that $\{, \}$ denotes the anticommutator. The notation indicates that after the usual approximations the matrix elements of \hat{C}^{in} and \hat{C}^{out} can be identified with the in-scattering and the out-scattering contributions to the collision integral in the Boltzmann equation which emerges from Eq. (A13) in the classical limit.

2. Distribution function

Another form of the kinetic equation can be obtained by expressing \hat{G}^K in terms of the distribution function \hat{g} by setting

$$\hat{G}^K = \hat{G}^R \hat{g}^\dagger - \hat{g} \hat{G}^A, \quad (\text{A16})$$

see Eq. (2.26). Note that a similar ansatz by Kamenev^{9,29} assumes that \hat{g} is hermitian, which in general is not correct. A formal proof that \hat{G}^K indeed can be written in

the form (2.26) can be found in Ref. [49] (see also Appendix B of Ref. [17]). The ansatz (A16) has some formal similarity to the generalized Kadanoff-Baym ansatz⁴⁹

$$G^K(t, t') = i[G^R(t, t')G^K(t', t') - G^K(t, t)G^A(t, t')], \quad (\text{A17})$$

which is often used to express the Keldysh Green function at different times in terms of its equal-time matrix elements. In fact, the generalized Kadanoff-Baym ansatz amounts to setting

$$[\hat{g}]_{tt'} = [\hat{g}^\dagger]_{t't} = \delta(t - t')iG^K(t, t). \quad (\text{A18})$$

Substituting Eq. (A16) into our definition (2.25) of the Keldysh self-energy $\hat{\Sigma}^K$, we obtain the kinetic equation

$$\hat{M}_0 \hat{g} - \hat{g}^\dagger \hat{M}_0 = -\hat{\Sigma}^K + \hat{\Sigma}^R \hat{g} - \hat{g}^\dagger \hat{\Sigma}^A, \quad (\text{A19})$$

which can also be written as [see Eq. (2.27)]

$$-i(\hat{M} \hat{g} - \hat{g}^\dagger \hat{M}) = \hat{\Sigma}^{\text{in}} - \hat{\Sigma}^{\text{out}}, \quad (\text{A20})$$

where $\hat{\Sigma}^{\text{in}}$ and $\hat{\Sigma}^{\text{out}}$ are defined in Eqs. (2.29, 2.30). Note that in the non-interacting limit or in a simple approximation where interaction corrections to the Keldysh self-energy $\hat{\Sigma}^K$ are neglected, we see from Eqs. (2.17a) and (2.25) that $\hat{\Sigma}^K$ reduces to an infinitesimal regularization $-i\eta(\hat{g} + \hat{g}^\dagger)$.

3. Wigner transformed Keldysh Green function

To describe the approach to equilibrium, it can be advantageous to perform a partial Fourier transformation of the two-time Green functions with respect to the time difference (Wigner transformation), see Eq. (2.33). Using the fact that

$$\begin{aligned} & [\hat{M}_0 \hat{G}^K - \hat{G}^K \hat{M}_0]_{tt'} = (i\partial_t + i\partial_{t'})G^K(t, t') \\ &= \int_{-\infty}^{\infty} \frac{d\omega}{2\pi} e^{-i\omega(t-t')} i\partial_\tau G^K(\tau; \omega), \end{aligned} \quad (\text{A21})$$

where $G^K(\tau; \omega)$ is the Wigner transform of $G^K(t, t')$, we obtain the following expression for the Wigner transform of our kinetic equation (A13) for the Keldysh Green function,

$$\begin{aligned} & i\partial_\tau G^K(\tau; \omega) - [\hat{\Sigma}^M, \hat{G}^K]_{(\tau; \omega)} - [\hat{\Sigma}^K, \hat{G}^M]_{(\tau; \omega)} \\ &= C^{\text{in}}(\tau; \omega) - C^{\text{out}}(\tau; \omega), \end{aligned} \quad (\text{A22})$$

where

$$C^{\text{in}}(\tau; \omega) = \frac{i}{2}\{\hat{\Sigma}^K, \hat{G}^I\}_{(\tau; \omega)}, \quad (\text{A23})$$

$$C^{\text{out}}(\tau; \omega) = \frac{i}{2}\{\hat{\Sigma}^I, \hat{G}^K\}_{(\tau; \omega)}. \quad (\text{A24})$$

Recall that the Wigner transform of the product of two matrices \hat{A} and \hat{B} in the time labels can be expressed in

terms of the Wigner transforms of the factors \hat{A} and \hat{B} as⁹

$$[\hat{A}\hat{B}]_{(\tau;\omega)} = \int ds_1 \int ds_2 \int \frac{d\omega_1}{2\pi} \int \frac{d\omega_2}{2\pi} e^{i(\omega_1 s_2 - \omega_2 s_1)} \times A\left(\tau + \frac{s_1}{2}; \omega + \omega_1\right) B\left(\tau + \frac{s_2}{2}; \omega + \omega_2\right). \quad (\text{A25})$$

Expanding the arguments of A and B for small $\omega_1, \omega_2, s_1, s_2$, and retaining only the first order in the derivatives we obtain the approximate expression

$$[\hat{A}\hat{B}]_{(\tau;\omega)} \approx A(\tau; \omega) B(\tau; \omega) + \frac{1}{2i} [\partial_\tau A(\tau; \omega) \partial_\omega B(\tau; \omega) - \partial_\omega A(\tau; \omega) \partial_\tau B(\tau; \omega)]. \quad (\text{A26})$$

Assuming that the τ -dependence of the distribution functions is slow, we may retain only the first term in the right-hand side of Eq. (A26), i.e. we approximate the Wigner transforms of the products appearing in the kinetic equations by the products of the Wigner transforms of the factors. In this approximation the Wigner transforms of the commutator terms on the left-hand side of the kinetic equation (A22) for $G^K(\tau; \omega)$ vanish, while the Wigner transforms of the collision integrals are

$$C^{\text{in}}(\tau; \omega) = i\Sigma^K(\tau; \omega)G^I(\tau; \omega), \quad (\text{A27})$$

$$C^{\text{out}}(\tau; \omega) = i\Sigma^I(\tau; \omega)G^K(\tau; \omega). \quad (\text{A28})$$

Given $G^K(\tau; \omega)$, we still have to perform a frequency integration to reconstruct the equal time Keldysh Green function (i.e. the distribution function),

$$G^K(t, t) = \int_{-\infty}^{\infty} \frac{d\omega}{2\pi} G^K(t; \omega). \quad (\text{A29})$$

4. Wigner transformed distribution function

We can avoid the above frequency integration by working with the Wigner transform $g_{\mathbf{k}}(\tau; \omega)$ of the kinetic equation (2.27) for the distribution matrix \hat{g} , which is given in Eq. (2.34). Note that in thermal equilibrium and in the absence of interactions the function $g_{\mathbf{k}}(\tau; \omega)$ is simply given by a symmetrized Bose function

$$g_{\mathbf{k}}(\tau; \omega) = 1 + \frac{2}{e^{\beta(\omega - \mu)} - 1} = \coth \left[\frac{\beta}{2}(\omega - \mu) \right]. \quad (\text{A30})$$

In an interacting system with well-defined quasi-particles, we expect that $g_{\mathbf{k}}(\tau; \omega)$ will relax towards a τ -independent function $g_{\mathbf{k}}(\omega)$ which for ω close to the renormalized quasi-particle energy can be expressed in terms of a symmetrized Bose function with some effective temperature. Using

$$\begin{aligned} [\hat{M}_0 \hat{g} - \hat{g}^\dagger \hat{M}_0]_{tt'} &= i\partial_t g_{tt'} + i\partial_{t'} g_{t't}^* - \epsilon_{\mathbf{k}}(g_{tt'} - g_{t't}^*) \\ &= \int_{-\infty}^{\infty} \frac{d\omega}{2\pi} e^{-i\omega(t-t')} \left[i\partial_\tau \text{Reg}(\tau; \omega) \right. \\ &\quad \left. + 2i(\omega - \epsilon_{\mathbf{k}}) \text{Im}g(\tau; \omega) \right], \end{aligned} \quad (\text{A31})$$

we finally arrive at Eq. (2.34).

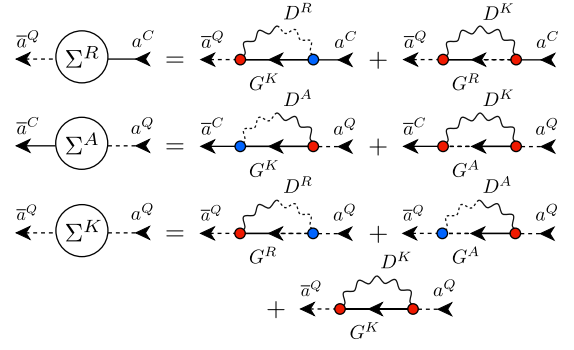


FIG. 6. (Color online) Diagrams contributing to the magnon self-energies to second order in the magnon-phonon coupling. The symbols are defined in the caption of Fig. 4.

APPENDIX B: SECOND ORDER SELF-ENERGIES

For the derivation of the perturbative kinetic equation (2.1) we need the components of the nonequilibrium self-energy to second order in the magnon-phonon coupling. In the contour-basis the self-energies are

$$\begin{aligned} \Sigma_{\mathbf{k}}^{pp'}(t, t') &= pp' \frac{i}{V} \sum_{\mathbf{q}} \gamma_{\mathbf{q}}^2 \left[D_{\mathbf{q}}^{pp'}(t, t') G_{\mathbf{k}-\mathbf{q}}^{pp'}(t, t') \right. \\ &\quad \left. + (\mathbf{q} \rightarrow -\mathbf{q}) \right]. \end{aligned} \quad (\text{B1})$$

Here the $p, p' \in \{+, -\}$ label the two branches of the Keldysh contour. Using the fact that the $(\mathbf{q} \rightarrow -\mathbf{q})$ term gives just a factor of 2 because the Green functions are even functions of the momentum argument, we obtain in the Keldysh basis

$$\begin{aligned} \Sigma_{\mathbf{k}}^R(t, t') &= \Sigma_{\mathbf{k}}^{QC}(t, t') = \frac{i}{V} \sum_{\mathbf{q}} \gamma_{\mathbf{q}}^2 \left[D_{\mathbf{q}}^R(t, t') G_{\mathbf{k}-\mathbf{q}}^K(t, t') \right. \\ &\quad \left. + D_{\mathbf{q}}^K(t, t') G_{\mathbf{k}-\mathbf{q}}^R(t, t') \right], \end{aligned} \quad (\text{B2a})$$

$$\begin{aligned} \Sigma_{\mathbf{k}}^A(t, t') &= \Sigma_{\mathbf{k}}^{CQ}(t, t') = \frac{i}{V} \sum_{\mathbf{q}} \gamma_{\mathbf{q}}^2 \left[D_{\mathbf{q}}^A(t, t') G_{\mathbf{k}-\mathbf{q}}^K(t, t') \right. \\ &\quad \left. + D_{\mathbf{q}}^K(t, t') G_{\mathbf{k}-\mathbf{q}}^A(t, t') \right], \end{aligned} \quad (\text{B2b})$$

$$\begin{aligned} \Sigma_{\mathbf{k}}^K(t, t') &= \Sigma_{\mathbf{k}}^{QQ}(t, t') = \frac{i}{V} \sum_{\mathbf{q}} \gamma_{\mathbf{q}}^2 \left[D_{\mathbf{q}}^K(t, t') G_{\mathbf{k}-\mathbf{q}}^K(t, t') \right. \\ &\quad \left. + D_{\mathbf{q}}^R(t, t') G_{\mathbf{k}-\mathbf{q}}^R(t, t') + D_{\mathbf{q}}^A(t, t') G_{\mathbf{k}-\mathbf{q}}^A(t, t') \right]. \end{aligned} \quad (\text{B2c})$$

The corresponding diagrams are shown in Fig. 6. The spectral component of the self-energy is

$$\begin{aligned} \Sigma_{\mathbf{k}}^I(t, t') &= i[\Sigma_{\mathbf{k}}^R(t, t') - \Sigma_{\mathbf{k}}^A(t, t')] \\ &= \frac{i}{V} \sum_{\mathbf{q}} \gamma_{\mathbf{q}}^2 \left[D_{\mathbf{q}}^I(t, t') G_{\mathbf{k}-\mathbf{q}}^K(t, t') \right. \\ &\quad \left. + D_{\mathbf{q}}^K(t, t') G_{\mathbf{k}-\mathbf{q}}^I(t, t') \right]. \end{aligned} \quad (\text{B3})$$

Moreover, using the fact that the product of a retarded and an advanced function with the same time argument

vanishes, the Keldysh component of the self-energy can alternatively be written as

$$\Sigma_{\mathbf{k}}^K(t, t') = \frac{i}{V} \sum_{\mathbf{q}} \gamma_{\mathbf{q}}^2 \left[D_{\mathbf{q}}^K(t, t') G_{\mathbf{k}-\mathbf{q}}^K(t, t') - D_{\mathbf{q}}^I(t, t') G_{\mathbf{k}-\mathbf{q}}^I(t, t') \right]. \quad (\text{B4})$$

To derive Wigner transformed kinetic equations, we use the fact that the Wigner transform of a product of two functions with the same time arguments can be written as a convolution in frequency space,

$$\begin{aligned} & [A(t, t')B(t, t')]_{(\tau, \omega)} \\ &= \int_{-\infty}^{\infty} ds e^{i\omega s} A\left(\tau + \frac{s}{2}, \tau - \frac{s}{2}\right) B\left(\tau + \frac{s}{2}, \tau - \frac{s}{2}\right) \\ &= \int_{-\infty}^{\infty} \frac{d\omega'}{2\pi} A(\tau; \omega') B(\tau; \omega - \omega'). \end{aligned} \quad (\text{B5})$$

The Wigner transform of the spectral and Keldysh components of our self-energies are therefore given by

$$\Sigma_{\mathbf{k}}^I(\tau; \omega) = \frac{i}{V} \sum_{\mathbf{q}} \int_{-\infty}^{\infty} \frac{d\omega'}{2\pi} \gamma_{\mathbf{q}}^2 \left[D_{\mathbf{q}}^I(\tau; \omega') G_{\mathbf{k}-\mathbf{q}}^K(\tau; \omega - \omega') + D_{\mathbf{q}}^K(\tau; \omega') G_{\mathbf{k}-\mathbf{q}}^I(\tau; \omega - \omega') \right], \quad (\text{B6})$$

$$\Sigma_{\mathbf{k}}^K(\tau; \omega) = \frac{i}{V} \sum_{\mathbf{q}} \int_{-\infty}^{\infty} \frac{d\omega'}{2\pi} \gamma_{\mathbf{q}}^2 \left[D_{\mathbf{q}}^K(\tau; \omega') G_{\mathbf{k}-\mathbf{q}}^K(\tau; \omega - \omega') - D_{\mathbf{q}}^I(\tau; \omega') G_{\mathbf{k}-\mathbf{q}}^I(\tau; \omega - \omega') \right]. \quad (\text{B7})$$

APPENDIX C: DERIVATION OF THE RATE EQUATION

In this appendix we summarize the approximations which are necessary to arrive at the perturbative kinetic equation (2.1). Using Eq. (2.26) we may express the Keldysh component of the Green function appearing on the right-hand side of Eqs. (B6, B7) in terms of the Wigner transform $g_{\mathbf{k}}(\tau; \omega)$ of the distribution function. To leading order in the gradients we may factorize the Wigner transform of the matrix products in Eq. (2.26),

$$iG_{\mathbf{k}}^K(\tau; \omega) \approx G_{\mathbf{k}}^I(\tau; \omega) g_{\mathbf{k}}(\tau; \omega). \quad (\text{C1})$$

After substituting the self-energies (B6) and (B7) with the Keldysh Green function given by Eq. (C1) into the Wigner transformed kinetic equation (2.38), we obtain an integro-differential equation for the nonequilibrium distribution function $g_{\mathbf{k}}(\tau) = g_{\mathbf{k}}(\tau; \omega = \epsilon_{\mathbf{k}})$. To further simplify this equation, let us assume that the phonon system is in thermal equilibrium. Moreover, we approximate the phonon propagators by the non-interacting equilibrium propagators. The Wigner transforms of the phonon Green functions can then be replaced by the usual Fourier

transforms,

$$F_{\mathbf{q}}^R(\omega) = \frac{1}{\omega - \omega_{\mathbf{q}} + i\eta}, \quad (\text{C2a})$$

$$F_{\mathbf{q}}^A(\omega) = \frac{1}{\omega - \omega_{\mathbf{q}} - i\eta}, \quad (\text{C2b})$$

$$F_{\mathbf{q}}^I(\omega) = i[F_{\mathbf{q}}^R(\omega) - F_{\mathbf{q}}^A(\omega)] = 2\pi\delta(\omega - \omega_{\mathbf{q}}), \quad (\text{C2c})$$

$$iF_{\mathbf{q}}^K(\omega) = \left[1 + \frac{2}{e^{\beta\omega} - 1} \right] F_{\mathbf{q}}^I(\omega) = f^0(\omega) F_{\mathbf{q}}^I(\omega), \quad (\text{C2d})$$

where

$$f^0(\omega) = 1 + \frac{2}{e^{\beta\omega} - 1} = \coth\left(\frac{\beta\omega}{2}\right) \quad (\text{C3})$$

is the equilibrium phonon distribution. The corresponding symmetrized phonon propagators are

$$\begin{aligned} D_{\mathbf{q}}^R(\omega) &= \frac{1}{2} [F_{\mathbf{q}}^R(\omega) + F_{-\mathbf{q}}^A(-\omega)] \\ &= \frac{\omega_{\mathbf{q}}}{(\omega + i\eta)^2 - \omega_{\mathbf{q}}^2}, \end{aligned} \quad (\text{C4a})$$

$$\begin{aligned} D_{\mathbf{q}}^A(\omega) &= \frac{1}{2} [F_{\mathbf{q}}^A(\omega) + F_{-\mathbf{q}}^R(-\omega)] \\ &= \frac{\omega_{\mathbf{q}}}{(\omega - i\eta)^2 - \omega_{\mathbf{q}}^2}, \end{aligned} \quad (\text{C4b})$$

$$\begin{aligned} D_{\mathbf{q}}^I(\omega) &= \frac{1}{2} [F_{\mathbf{q}}^I(\omega) - F_{-\mathbf{q}}^I(-\omega)] \\ &= \pi \text{sgn}(\omega) [\delta(\omega - \omega_{\mathbf{q}}) + \delta(\omega + \omega_{\mathbf{q}})], \end{aligned} \quad (\text{C4c})$$

$$iD_{\mathbf{q}}^K(\omega) = \frac{i}{2} [F_{\mathbf{q}}^K(\omega) + F_{-\mathbf{q}}^K(-\omega)] \quad (\text{C4d})$$

$$= f^0(\omega) D_{\mathbf{q}}^I(\omega). \quad (\text{C4e})$$

Substituting Eqs. (C1) and (C4e) into Eqs. (B6) and (B7) we obtain for the in-scattering and out-scattering components of the nonequilibrium self-energy

$$\begin{aligned} \Sigma_{\mathbf{k}}^{\text{in}}(\tau; \omega) &= i\Sigma_{\mathbf{k}}^K(\tau; \omega) \\ &= \frac{1}{V} \sum_{\mathbf{q}} \gamma_{\mathbf{q}}^2 \int_{-\infty}^{\infty} \frac{d\omega'}{2\pi} D_{\mathbf{q}}^I(\omega') G_{\mathbf{k}-\mathbf{q}}^I(\tau; \omega - \omega') \\ &\quad \times [f^0(\omega') g_{\mathbf{k}-\mathbf{q}}(\tau; \omega - \omega') + 1], \end{aligned} \quad (\text{C5})$$

$$\begin{aligned} \Sigma_{\mathbf{k}}^{\text{out}}(\tau; \omega) &= \Sigma_{\mathbf{k}}^I(\tau; \omega) g_{\mathbf{k}}(\tau; \omega) \\ &= \frac{1}{V} \sum_{\mathbf{q}} \gamma_{\mathbf{q}}^2 \int_{-\infty}^{\infty} \frac{d\omega'}{2\pi} D_{\mathbf{q}}^I(\omega') G_{\mathbf{k}-\mathbf{q}}^I(\tau; \omega - \omega') \\ &\quad \times [f^0(\omega') + g_{\mathbf{k}-\mathbf{q}}(\tau; \omega - \omega')] g_{\mathbf{k}}(\tau; \omega). \end{aligned} \quad (\text{C6})$$

Combining in- and out scattering contributions to the collision integral, we obtain the quantum kinetic equation

$$\begin{aligned} \partial_{\tau} g_{\mathbf{k}}(\tau; \omega) &= \frac{1}{V} \sum_{\mathbf{q}} \gamma_{\mathbf{q}}^2 \int_{-\infty}^{\infty} \frac{d\omega'}{2\pi} D_{\mathbf{q}}^I(\omega') G_{\mathbf{k}-\mathbf{q}}^I(\tau; \omega - \omega') \\ &\quad \times \left\{ f^0(\omega') [g_{\mathbf{k}-\mathbf{q}}(\tau; \omega - \omega') - g_{\mathbf{k}}(\tau; \omega)] \right. \\ &\quad \left. + 1 - g_{\mathbf{k}-\mathbf{q}}(\tau; \omega - \omega') g_{\mathbf{k}}(\tau; \omega) \right\}. \end{aligned} \quad (\text{C7})$$

In thermal equilibrium the different components of the magnon Green function satisfy the fluctuation-dissipation theorem, which is equivalent with

$$g_{\mathbf{k}}(\tau; \omega) \rightarrow \coth\left(\frac{\beta(\omega - \mu)}{2}\right) = g^0(\omega). \quad (\text{C8})$$

Using the identity

$$\coth(x - y) = \frac{1 - \coth x \coth y}{\coth x - \coth y}, \quad (\text{C9})$$

with $x = \beta(\omega - \mu)/2$ and $y = \beta\omega'/2$ it is easy to see that in thermal equilibrium the in- and out-scattering contributions cancel, so that the right-hand side of Eq. (C7) vanishes identically.

To reduce Eq. (C7) to the rate equation (2.1) we set

$$g_{\mathbf{k}}(\tau; \omega) = 1 + 2n_{\mathbf{k}}(\tau; \omega), \quad (\text{C10})$$

$$f^0(\omega) = 1 + 2b(\omega) = 1 + \frac{2}{e^{\beta\omega} - 1}, \quad (\text{C11})$$

and shift the phonon momentum, $\mathbf{q} = \mathbf{k} - \mathbf{k}'$. Then

Eq. (C7) can be written as

$$\begin{aligned} \partial_{\tau} n_{\mathbf{k}}(\tau; \omega) = & \frac{1}{V} \sum_{\mathbf{k}'} \int_{-\infty}^{\infty} \frac{d\omega'}{2\pi} 2\gamma_{\mathbf{k}-\mathbf{k}'}^2 D_{\mathbf{k}-\mathbf{k}'}^I(\omega - \omega') \\ & \times G_{\mathbf{k}'}^I(\tau; \omega') \left\{ [1 + n_{\mathbf{k}}(\tau; \omega)] b(\omega - \omega') n_{\mathbf{k}'}(\tau; \omega') \right. \\ & \left. + [1 + n_{\mathbf{k}'}(\tau; \omega')] b(\omega' - \omega) n_{\mathbf{k}}(\tau; \omega) \right\}. \end{aligned} \quad (\text{C12})$$

Finally, we neglect the damping of intermediate states, which amounts to approximating

$$G_{\mathbf{k}'}^I(\tau; \omega') \approx 2\pi\delta(\omega' - \epsilon_{\mathbf{k}'}). \quad (\text{C13})$$

Then the ω' -integration in Eq. (C12) is trivial and we obtain for $n_{\mathbf{k}}(\tau) = n_{\mathbf{k}}(\tau; \epsilon_{\mathbf{k}})$ the kinetic equation

$$\begin{aligned} \partial_{\tau} n_{\mathbf{k}}(\tau) = & \frac{2}{V} \sum_{\mathbf{k}'} \gamma_{\mathbf{k}-\mathbf{k}'}^2 D_{\mathbf{k}-\mathbf{k}'}^I(\epsilon_{\mathbf{k}} - \epsilon_{\mathbf{k}'}) \\ & \times \left\{ [1 + n_{\mathbf{k}}(\tau)] b(\epsilon_{\mathbf{k}} - \epsilon_{\mathbf{k}'}) n_{\mathbf{k}'}(\tau) \right. \\ & \left. - [1 + n_{\mathbf{k}'}(\tau)] [1 + b(\epsilon_{\mathbf{k}} - \epsilon_{\mathbf{k}'})] n_{\mathbf{k}}(\tau) \right\}. \end{aligned} \quad (\text{C14})$$

This is of the form (2.1) with transition rates $W_{\mathbf{k}, \mathbf{k}'}$ given by Eq. (2.2).

-
- ¹ K. Morawetz (ed.), *Nonequilibrium Physics at Short Time Scales*, (Springer, Berlin, 2004).
- ² A. Polkovnikov, K. Sengupta, A. Silva, and M. Vengalattore, *Rev. Mod. Phys.* **83**, 863 (2011).
- ³ W. Cassing, *Eur. Phys. J. Special Topics* **168**, 3 (2009).
- ⁴ H. Deng, H. Haug, and Y. Yamamoto, *Rev. Mod. Phys.* **82**, 1489 (2010).
- ⁵ H. Schoeller, *Eur. Phys. J. Special Topics* **168**, 179 (2009).
- ⁶ S. O. Demokritov, V. E. Demidov, O. Dzyapko, G. A. Melkov, A. A. Serga, B. Hillebrands, and A. N. Slavin, *Nature* **443**, 430 (2006).
- ⁷ O. Dzyapko, V. E. Demidov, G. A. Melkov, and S. O. Demokritov, *Phil. Trans. R. Soc. A* **369**, 3575 (2011).
- ⁸ A. Griffin, T. Nikuni, and E. Zaremba, *Bose-Condensed Gases at Finite Temperature*, (Cambridge University Press, Cambridge, 2009).
- ⁹ A. Kamenev, *Field Theory of Nonequilibrium Systems* (Cambridge University Press, Cambridge, 2011).
- ¹⁰ J. Berges and G. Hoffmeister, *Nucl. Phys. B* **813**, 383 (2009); J. Berges and D. Sexty, *Phys. Rev. D* **83**, 085004 (2011); J. Berges and D. Sexty, *Phys. Rev. Lett.* **108**, 161601 (2012).
- ¹¹ C. Bagnuls and C. Bervillier, *Phys. Rep.* **348**, 91 (2001).
- ¹² J. Berges, N. Tetradis, and C. Wetterich, *Phys. Rep.* **363**, 223 (2002).
- ¹³ P. Kopietz, L. Bartosch, and F. Schütz, *Introduction to the Functional Renormalization Group* (Springer, Berlin, 2010).
- ¹⁴ O. J. Rosten, *Phys. Rep.* **511**, 177 (2012).
- ¹⁵ W. Metzner, M. Salmhofer, C. Honerkamp, V. Meden, and K. Schönhammer, *Rev. Mod. Phys.* **84**, 299 (2012).
- ¹⁶ T. Gasenzer and J. M. Pawłowski, *Phys. Lett. B* **670**, 135 (2008); T. Gasenzer, S. Keßler, and J. M. Pawłowski, *Eur. Phys. J. C* **70**, 423 (2010).
- ¹⁷ T. Kloss and P. Kopietz, *Phys. Rev. B* **83**, 205118 (2011).
- ¹⁸ D. M. Kennes, S. G. Jakob, C. Karrasch, and V. Meden, *Phys. Rev. B* **85**, 085113 (2012).
- ¹⁹ See, for example, A. L. Fetter and J. D. Walecka, *Quantum Theory of Many-Particle Systems* (McGraw-Hill, New York, 1971).
- ²⁰ L. Bányai, P. Gartner, O. M. Schmitt, and H. Haug, *Phys. Rev. B* **61**, 8823 (2000).
- ²¹ V. Cherepanov, I. Kolokolov, and V. L'vov, *Phys. Rept.* **229**, 81 (1993).
- ²² V. E. Demidov, O. Dzyapko, S. O. Demokritov, G. A. Melkov, and A. N. Slavin, *Phys. Rev. Lett.* **100**, 047205 (2008).
- ²³ V. E. Demidov, O. Dzyapko, M. Buchmeier, T. Stockhoff, G. Schmitz, G. A. Melkov, and S. O. Demokritov, *Phys. Rev. Lett.* **101**, 257201 (2008).
- ²⁴ A. Kreisel, F. Sauli, L. Bartosch, and P. Kopietz, *Eur. Phys. J. B* **71**, 59 (2009).
- ²⁵ B. A. Kalinikos and A. N. Slavin, *J. Phys. C* **19**, 7013 (1986); B. A. Kalinikos, M. P. Kostylev, N. V. Kozhus, and A. N. Slavin, *J. Phys. Condens. Matter* **2**, 9861 (1990).
- ²⁶ J. Hick, F. Sauli, A. Kreisel, and P. Kopietz, *Eur. Phys. J. B* **78**, 429 (2010).
- ²⁷ Note that our transition rates $W_{\mathbf{k}, \mathbf{k}'}$ correspond to $W_{\mathbf{k}', \mathbf{k}}$ (with interchanged momentum labels) of Ref. [20]. We follow here the convention of the textbook by R. Zwanzig, *Nonequilibrium Statistical Mechanics* (Oxford University Press, Oxford, 2001).

- ²⁸ J. W. Negele and H. Orland, *Quantum Many-Particle Systems* (Addison-Wesley, Redwood City, 1988).
- ²⁹ A. Kamenev, in *Les Houches, Volume Session LX*, edited by H. Bouchiat, Y. Gefen, S. Guéron, G. Montambaux, and J. Dalibard (Elsevier, North-Holland, Amsterdam, 2004).
- ³⁰ As explained, for example by Kamenev^{9,29}, in a functional integral formalism it is natural to parametrize the nonequilibrium Green functions in the Keldysh basis and to work with the three independent Green functions G^R , G^A and G^K . The Kadanoff-Baym parametrization corresponds to the contour basis, with $G^> = G^{-+}$ and $G^< = G^{+-}$, where $iG_k^{pp'}(t, t') = \langle a_k^p(t) \bar{a}_k^{p'}(t') \rangle$ with $p, p' \in \{+, -\}$.
- ³¹ P. Danielewicz, *Ann. Phys.* **152**, 239 (1984).
- ³² D. Semkat, D. Kremp, and M. Bonitz, *J. Math. Phys.* **41**, 7458 (2000).
- ³³ M. Garny and M. M. Müller, *Phys. Rev. D* **80**, 085011 (2009).
- ³⁴ J. Rammer, *Quantum Field Theory of Nonequilibrium States* (Cambridge University Press, Cambridge, 2007).
- ³⁵ C. Wetterich, *Phys. Lett. B* **301**, 90 (1993).
- ³⁶ S. G. Jakobs, M. Pletyukhov, and H. Schoeller, *Phys. Rev. B* **81**, 195109 (2010); S. G. Jakobs, M. Pletyukhov, and H. Schoeller, *J. Phys. A: Math. Theor.* **43**, 103001 (2010); C. Karrasch, M. Pletyukhov, L. Borda, and V. Meden, *Phys. Rev. B* **81**, 125122 (2010).
- ³⁷ F. Schütz, L. Bartosch, and P. Kopietz, *Phys. Rev. B* **72**, 035107 (2005); F. Schütz and P. Kopietz, *J. Phys. A: Math. Gen.* **39**, 8205 (2006).
- ³⁸ T. Jolicœur and J. C. Le Guillou, *Phys. Rev. B* **44**, 2403 (1991).
- ³⁹ C. W. Sandweg, M. B. Jungfleisch, V. I. Vasyuchka, A. A. Serga, P. Clausen, H. Schultheiss, B. Hillebrands, A. Kreisel, and P. Kopietz, *Rev. Sci. Instrum.* **81**, 073902 (2010).
- ⁴⁰ D. Snoke, *Nature* **443**, 403 (2006).
- ⁴¹ A. I. Bugrij and V. M. Loktev, *Low Temp. Phys.* **33**, 37 (2007)
- ⁴² A. Rückriegel, A. Kreisel, and P. Kopietz, *Phys. Rev. B* **85**, 054422 (2012).
- ⁴³ W. Kohn and D. Sherrington, *Rev. Mod. Phys.* **42**, 1 (1970).
- ⁴⁴ O. Jepsen, J. Madsen, and O. K. Andersen, *Phys. Rev. B* **18**, 605 (1978).
- ⁴⁵ G. G. Siu, C. M. Lee, and Y. Liu, *Phys. Rev. B* **64**, 094421 (2001).
- ⁴⁶ A. L. Chernyshev, *Phys. Rev. B* **86**, 060401(R) (2012).
- ⁴⁷ A. Kreisel, P. Kopietz, P. T. Cong, B. Wolf, and M. Lang, *Phys. Rev. B* **84**, 024414 (2011).
- ⁴⁸ Note that in Ref. [20] Bányai *et al.* use a decoupling procedure to derive an equation of motion for the order parameter $\psi_0(t) = \langle a_{\mathbf{k}=0}(t) \rangle$. It is easy to see that in our notation their order parameter equation can be written as $i\partial_t \psi_0(t) = \Sigma_{\mathbf{k}=0}^R(t; \omega = 0) \psi_0(t)$, where $\Sigma_{\mathbf{k}}^R(\tau; \omega)$ is the Wigner transform of the retarded self-energy to second order in the magnon-phonon coupling, see Eq. (B2a). This equation can be viewed as a linearized Gross-Pitaevskii equation. For a consistent description of the condensed phase, the non-linear terms in the Gross-Pitaevskii equation should be retained. These terms arise from magnon-magnon interactions which we have neglected in our model Hamiltonian defined in Eq. (1.1).
- ⁴⁹ P. Lipavský, V. Špička, and B. Velický, *Phys. Rev. B* **34**, 6933 (1986).